

Modernization of monoclonal antibody screening and protein-interaction assays

Thesis by
Michael Aurelio Anaya

In Partial Fulfillment of the Requirements for the
Degree of
Doctor of Philosophy

The logo for the California Institute of Technology (Caltech), featuring the word "Caltech" in a bold, orange, sans-serif font.

CALIFORNIA INSTITUTE OF TECHNOLOGY
Pasadena, California

2021
Defended March 2, 2021

© 2021

Michael Aurelio Anaya
ORCID: 0000-0002-6944-3614

All rights reserved

ACKNOWLEDGEMENTS

For my brother, Mark. I wish you were still here.

ABSTRACT

In this research, multiplexed bead-based technology was employed to develop a high-throughput monoclonal antibody production method and to refine a protein-protein interaction (PPI) assay for interactome screening. Hybridoma supernatants produced from mice injected with multiple antigens were screened with color-coded, antigen-coupled beads in a semi-automated workflow. Two monoclonal antibodies, each demonstrating high specificity and strong binding, were produced. To our knowledge, these results are the first demonstrated usage of multiplexed suspension bead-based screening as a critical component of high-throughput antibody production. The technology was also utilized as a PPI assay due to its numerous advantages over ELISA-based screens. We studied interactions of the extracellular domains of the Beat and Side protein families, whose members control neuromuscular specificity in *Drosophila melanogaster* and form a highly-connected interaction network. We demonstrated that a screen utilizing avidin-captured bait was superior to a screen utilizing Protein A-captured bait and deorphanized five proteins within the network, namely Beat 1b, Beat 3a, Beat 3c, Side 5, and Side 8.

PUBLISHED CONTENT AND CONTRIBUTIONS

Menon, Kaushiki P., Vivek Kulkarni, Shin-Ya Takemura, Michael Anaya, and Kai Zinn (2019). “Interactions between Dpr11 and DIP- γ control selection of amacrine neurons in *Drosophila* color vision circuits”. In: *eLife* 8. DOI: 10 . 7554/eLife.48935.

MA prepared reagents used in the study, participated in discussions on the project, and reviewed the manuscript.

Li, Hanqing, Ash Watson, Agnieszka Olechwier, Michael Anaya, Siamak K. Sorooshyari, Dermott P. Harnett, Hyung-Kook Peter Lee, Jost Vielmetter, Mario A. Fares, K. Christopher Garcia, Engin Özkan, Juan-Pablo Labrador, and Kai Zinn (2017). “Deconstruction of the beaten Path-Sidestep interaction network provides insights into neuromuscular system development”. In: *eLife* 6. DOI: 10 . 7554 / eLife.28111.

MA participated in the conception of the project, assisted with experimental design and execution, and reviewed the manuscript.

TABLE OF CONTENTS

Acknowledgements	iii
Abstract	iv
Published Content and Contributions	v
Table of Contents	vi
Chapter I: Introduction	1
Chapter II: In-depth analysis of multiplexed bead-based assays	3
2.1 Background	3
2.2 Introduction	5
2.3 Materials and Methods	6
2.4 Results	6
Chapter III: High-throughput monoclonal antibody production	18
3.1 Background	18
3.2 Introduction	20
3.3 Materials and Methods	21
3.4 Results	25
3.5 Discussion	33
Chapter IV: Multiplexed bead-based interactome screening	37
4.1 Background	37
4.2 Introduction	39
4.3 Materials and Methods	40
4.4 Results	43
4.5 Discussion	50
Bibliography	53

Chapter 1

INTRODUCTION

The progress of human civilization is largely characterized, if not defined, by the advancement of technology. From the Stone Age to the Information Age, technological achievement has demarcated the successive periods of our development. The three pillars of knowledge and expression, namely philosophy, art, and science, have been fundamentally transformed by technology in dramatic and meaningful ways. Photographs such as “Earthrise,” “Pale Blue Dot,” and “Hubble Deep Field” were made possible by a combination of technologies including rocketry and optics. These images captured the world’s imagination and provided humanity with new perspectives about our place in the cosmos. The field of biology has also been radically changed by technology. The quintessential scientific instrument known as the microscope introduced us to the microscale universe through the discovery of cells and microorganisms, and structure visualization at nanometer and sub-nanometer scale is the current forefront of structural biology.

Multiplexing and high-throughput assays are two manifestations of technology’s continued impact on modern biology. Multiplexing, as it applies to molecular biology, refers to the ability to probe a single sample with multiple analytes. High-throughput assays, on the other hand, are experiments in which a substantial number of samples are analyzed either simultaneously or sequentially. There are no formal guidelines for qualifying as high-throughput. Automation via computers and robotic control systems such as liquid handlers typically underlie high-throughput methods. Multiplexing may also be utilized to achieve high-throughput capacity, but not all high-throughput processes employ multiplexing as a pipeline component. Therefore, the two terms are related but not interchangeable.

Multiplex and high-throughput methodologies have revolutionized molecular biology by reducing the amount of time, labor, and resources required to conduct experiments while expanding the scale of such experiments by several orders of magnitude. The Human Genome Project (HGP) was an international research project with the objective of sequencing the entire 3 Gbp human genome. This monumental effort took a coalition of scientists from academic, government, and private sectors nearly a decade to complete and culminated in 2001 (International

Human Genome Sequencing Consortium et al., 2001; Venter et al., 2001). It remains the world's largest collaborative biological project. However, high-throughput sequencing, also known as next generation sequencing (NGS), now enables a human genome to be sequenced within a single day at a tiny fraction of the cost of the HGP (Behjati and Tarpey, 2013). NGS is even being utilized in a massively scaled up screen for severe acute respiratory syndrome coronavirus 2 (SARS-CoV-2) in saliva samples using a technique known as SwabSeq (J. S. Bloom et al., 2020).

The enzyme-linked immunosorbent assay (ELISA) has become the gold standard for protein interaction assays since its invention in 1971 (Engvall and Perlmann, 1971). Despite the technique's ubiquity, it is not trivial to scale up. The number of wells required to screen a collection of n bait proteins by m prey proteins is given by nm . Proteins can be pooled into single wells as baits or preys to reduce reagent consumption and to improve throughput of the assay format. A pooled-bait strategy is described in this work as a solution for ELISA-based high-throughput monoclonal antibody screening, and a pooled-prey strategy was recently employed successfully in an interactome screen of 564 human cell-surface and secreted proteins (Wojtowicz, Vielmetter, et al., 2020). However, pooling strategies suffer from two major drawbacks – dilution of the baits and/or preys and necessitating subsequent deconvolution assays. Since the sensitivity of an ELISA is directly related to the concentrations of bait and prey proteins, diluting either of them increases the risk of failing to detect the interaction. Furthermore, deconvolution strategies are only helpful if the majority of wells produce a negative result in the initial screen.

Multiplexed bead-based arrays allow up to 500 analytes to be covalently-coupled onto uniquely identifiable microspheres and pooled, thereby eliminating the two significant drawbacks of plate-based, high-throughput ELISA screening. In this format, the number of wells required to screen a collection of n bait proteins by m prey proteins is $\lceil \frac{n}{x} \rceil \times m$, where x is 50, 100, or 500 (depending on the instrument) and $\lceil \frac{n}{x} \rceil$ denotes the least integer that is greater than or equal to $\frac{n}{x}$. Using a multiplexed bead-based array, a collection of 564 proteins could be screened against itself on as few as three 384-well plates using as little as 60 μL of each prey.

Chapter 2

IN-DEPTH ANALYSIS OF MULTIPLEXED BEAD-BASED ASSAYS

2.1 Background

Robust multiplexed bead-based assays emerged in the 1990s as the result of a unification of several disparate technologies into a single platform. Although many of the core components of these assays were available in the 1970s, namely flow cytometers, antibodies, and microspheres, other technologies needed further development to enable their commercialization. The advent of diode lasers, avalanche photodiodes and pulse profile measurements, coupled with an increasing diversity of antibodies, dyes and lasers, enabled the realization of multicolor analysis at cheaper and faster scales than ever before (Graham, Chandler, and Dunbar, 2019). The exponential growth of computing power accomplished during this time period permitted the real-time processing of the enormous amounts of data generated by these assays.

The idea of using differentially colored beads as a means for multiplexing was suggested by a computer scientist during lunch at a Mexican restaurant in Texas in 1994 and spurred the formation of the Luminex Corporation (Graham, Chandler, and Dunbar, 2019). Over time, the company evolved from simply providing reagents to be used on existing flow cytometers to offering full-fledged solutions incorporating reagents, instrumentation, and software. The company currently offers three lines of instruments, differentiated primarily by the number of color-coded beads each instrument can simultaneously process. The Luminex MAGPIX has a multiplex capacity of 50, whereas the Luminex 100/200 and Luminex FLEXMAP 3D have multiplex capacities of 100 and 500, respectively. Furthermore, the company has licensed the technology to several other industry partners, resulting in the following (non-comprehensive) list of co-branded instruments: Perkin-Elmer CS1000 Autoplex Analyzer, Qiagen Liquichip, Linco Research Lincoplex 200, Fisher Scientific Prima, **One Lambda LabScan100** and **LabScan 3D**, **Zeus Athena Multi-Lyte**, **Millipore Milliplex Analyzer**, **Immucor Immucor LX200** (a.k.a. GenProbe LX200), and **Bio-Rad Bio-Plex 200**, **Bio-Plex 3D**, and MAGPIX (D. Vlassov, personal communication). (Note: Instruments listed in bold are extant at the time of

writing.) The Caltech Protein Expression Center acquired a Bio-Rad Bio-Plex 200 in February 2015, and this instrument was used to perform all bead-based experiments described herein. The Bio-Plex 200 is capable of simultaneously analyzing up to 80 magnetic or 100 non-magnetic bead colors, also known as bead regions.

Color-coding of the beads is the key aspect enabling the ability to multiplex in these assays. During the time of manufacture, each batch of beads is infused with a specific ratio of two or three dyes. When probed with a laser of an appropriate wavelength, each ratio produces a spectrally distinct emission profile. By optimizing the ratios of the infusion dyes and developing algorithms to deconvolute their emission profiles, Luminex developed the capability of creating up to 100 unique bead regions using two dyes and up to 500 unique bead regions using three dyes. Another aspect of the technology is the ability to covalently link biomolecules to the surface of the beads. For custom assays, beads are functionalized with carboxyl (-COOH) groups on their surface to allow for covalent coupling of biomolecules bearing a primary amine (-NH₂) via carbodiimide crosslinking chemistry. Alternatively, commercial bead sets are available to the research community in which beads have already been coupled to capture proteins or antibodies and pooled to create a ready-to-use multiplexed bead set.

One of the earliest publications demonstrating the applicability of this technology to the biological sciences occurred in 1997. Operating under the brand name FlowMetrix™ at that time, Fulton and colleagues at Luminex Corp. developed an assay to measure canine serum levels of IgGs and IgEs against 16 different grass allergens as well as an oligonucleotide-based assay to perform HLA-DQA1 tissue-typing on PCR-amplified human genomic DNA (Fulton et al., 1997). Thus, two major classes of biomolecules, proteins and nucleic acids, were shown to be efficiently interrogated from biological samples in a single publication. Two technical analyses were subsequently published in 1998, focusing primarily on the spectral properties forming the basis of the bead classification system, by scientists at Luminex and Los Alamos National Laboratory (Kettman Jr et al., 1998; Keij and Steinkamp, 1998).

The most common usage of multiplexed bead-based assays is the measurement of cytokines and cytokine-associated biomarkers. Because there are many members within the cytokine family and multiple cytokines are expressed and secreted simultaneously in response to particular stimuli, assays that can measure the levels of multiple cytokines at once provide a more thorough analysis of the underlying biol-

ogy of the process being studied. These assays are typically designed as a capture sandwich immunoassay. In this format, capture antibodies are covalently-coupled to microspheres, and the microspheres are then exposed to a biological sample containing the analytes. Biotinylated detection antibodies, which bind to different epitopes on the analytes than the capture antibodies, are then used to detect the bound analytes, if present. Lastly, fluorescently-labeled streptavidin is applied in order to label the beads with a fluorescent reporter. The beads are then interrogated by two lasers within the instrument – one laser to determine the bead color, corresponding to the analyte being measured, and one laser to detect the fluorescent reporter, with the intensity of fluorescence being directly correlated to the concentration of the analyte in the sample. An early variant of this assay, using fluorescently-labeled detection antibodies instead of biotinylated antibodies followed by fluorescently-labeled streptavidin, was used to detect the human cytokines granulocyte macrophage colony-stimulating factor (GM-CSF), interleukin-2 (IL-2), interleukin-4 (IL-4), and tumor necrosis factor- α (TNF- α) and was published in 1998 by scientists at Luminex (Oliver, Kettman, and Fulton, 1998). Publications describing the 2-step detection strategy described above followed shortly thereafter (Carson and Vignali, 1999; Vignali, 2000). The 2-step detection method has effectively replaced the usage of fluorescently-labeled antibodies in commercially available kits.

2.2 Introduction

Custom Bio-Plex assays provide maximum freedom to researchers in terms of choice of analytes and detection strategies. Yet they present a challenge in that all of the relevant assay parameters, such as coupling concentrations, limits of detection and saturation, and range of signal, must be determined prior to their application to address a research question. Unlike commercial bead sets, where beads have already been coupled to capture reagents or analytes of interest and then combined to ensure equal representation of each bead region in the final multiplexed bead mixture, custom assays necessitate that the end-user perform this task. Furthermore, standards containing the analytes of interest are provided in well-defined concentrations in commercial kits, facilitating the creation of standard curves that can be used to quantify unknown samples. However, in some cases, such standards are unavailable or impractical for custom assays, especially for those designed for a purpose beyond measuring the concentration of target analytes in a sample.

This chapter describes many of the lessons gleaned during the development of

custom Bio-Plex assays. These experiments illuminate several of the fundamental properties of the Bio-Plex 200 system, many of which are not discussed or are only superficially mentioned in the user manual. Hopefully, future scientists will be encouraged to develop their own assays utilizing the technology in new and creative ways while decreasing their reliance on commercial kits.

2.3 Materials and Methods

Bead validation assays. For bead region classification experiments, 0.5 μL of vortexed magnetic Bio-Plex beads at approximately 12,500 beads per μL were pipetted into individual wells of a low-profile 96-well plate (Bio-Rad Laboratories Cat. HSP9631) containing 100 μL of 1x PBS. The Bio-Plex 200 was set to report on all 80 of the compatible magnetic bead regions and read method was set to “total classified” with an input value of 1,000.

Bead coupling and staining protocol. Avidin (Sigma-Aldrich Cat. A9275) and streptavidin (Sigma-Aldrich Cat. S4762) were coupled to 50,000 beads each at concentrations of 5 ng/ μL , 10 ng/ μL , 20 ng/ μL and 40 ng/ μL . Protein A (Rockland™ Antibodies and Assays Cat. PA00-00) was coupled to 125,000 beads at a concentration of 2.4 ng/ μL . Beads were blocked in 5% (w/v) BSA blocking buffer prepared from lyophilized BSA (Rockland™ Antibodies and Assays Cat. BSA-1000) in TBST with 0.01% (w/v) thimerosal. Avidin- and streptavidin-coupled beads were incubated with 100 μL of biotinylated goat (anti-Rabbit IgG) IgG (Vector Labs Cat. BA-1000) at 2 ng/ μL in 5% (w/v) BSA blocking buffer. Protein A-coupled beads were incubated with chemically-biotinylated recombinant human anti-H3N2 HA antibody (C05) (Creative BioLabs Cat. PABZ-198) at 2 ng/ μL in 5% (w/v) BSA blocking buffer or non-biotinylated human IgG1 (Sigma-Aldrich Cat. I5154) at 2 ng/ μL in 5% (w/v) BSA blocking buffer. Streptavidin-phycoerythrin (Bio-Rad Laboratories Cat. 171-304501, or BioLegend Cat. 405203) was used at 1x (Bio-Rad) or 4 ng/ μL (BioLegend) in 5% (w/v) BSA blocking buffer or 1x PBS as the fluorescent reporter for the assay. Expi293™ Expression Medium (ThermoFisher Scientific Cat. A14351-01) and Schneider’s Drosophila Medium (ThermoFisher Scientific Cat. 21720-024) was collected by harvesting the supernatant of cell cultures after 3-4 days of growth.

2.4 Results

Bead region classification. The Bio-Plex 200 is able to distinguish up to 100 unique bead regions if the beads are non-magnetic and up to 80 unique bead regions if the

beads are magnetic. Having acquired all 80 of the magnetic bead regions compatible with the Bio-Plex 200, we sought to determine the efficiency of the instrument's bead region classification. Approximately 6,250 beads of each region were pipetted into individual wells of a 96-well plate and then processed by the Bio-Plex 200 using the "total classified" read method set to 1,000. Bead count data were analyzed across all 80 regions (Figure 2.1). For each well, the highest bead count was observed in the labeled region. Classify efficiency, defined as the ratio of the bead count in the labeled bead region to the total bead count within a well, ranged from 95% to 99.1% and had a mean of 97.6% (Figure 2.2). The manufacturer has specified Classify efficiency of >80% as the threshold to pass the Classify Validation portion of instrument validation. Therefore, the results above confirmed that all of the bead regions exceeded the threshold.

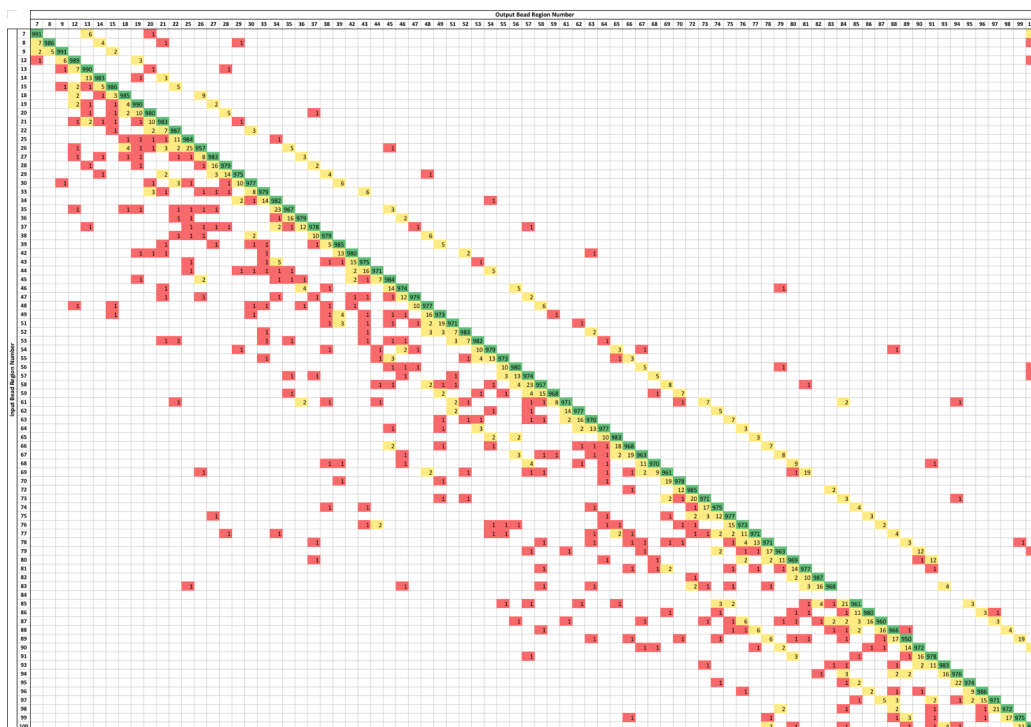


Figure 2.1: 80 x 80 bead count matrix. All 80 magnetic bead regions compatible with the Bio-Plex 200 were pipetted into separate wells and then read on the Bio-Plex 200. A 3-color scale was applied to the data, where green represents bead counts ≥ 950 , yellow represents bead counts between 2 and 25, and red represents a bead count of 1.

Bead counts in regions not corresponding to the labeled region were consistently observed at an average rate of 2.4% (Figure 2.2). These off-target counts are the result of two phenomena: bead carryover and systematic misclassification. Bead

Region	Region bead count	Total Bead Count	% on-target	% off-target	Carryover bead count	% off-target due to carryover
7	991	1000	99.1	0.9		
8	986	1000	98.6	1.4	7	0.7
9	991	1000	99.1	0.9	5	0.5
12	989	1000	98.9	1.1	6	0.6
13	990	1000	99.0	1.0	7	0.7
14	983	1000	98.3	1.7	13	1.3
15	986	1000	98.6	1.4	5	0.5
18	985	1000	98.5	1.5	3	0.3
19	990	1000	99.0	1.0	4	0.4
20	980	1000	98.0	2.0	10	1.0
21	983	1000	98.3	1.7	10	1.0
22	987	1000	98.7	1.3	7	0.7
25	984	1000	98.4	1.6	11	1.1
26	957	1000	95.7	4.3	25	2.5
27	983	1000	98.3	1.7	8	0.8
28	979	1000	97.9	2.1	16	1.6
29	975	1000	97.5	2.5	14	1.4
30	977	1000	97.7	2.3	10	1.0
33	979	1000	97.9	2.1	8	0.8
34	982	1000	98.2	1.8	14	1.4
35	967	1000	96.7	3.3	23	2.3
36	979	1000	97.9	2.1	16	1.6
37	978	1000	97.8	2.2	12	1.2
38	979	1000	97.9	2.1	10	1.0
39	985	1000	98.5	1.5	5	0.5
42	980	1000	98.0	2.0	13	1.3
43	975	1000	97.5	2.5	15	1.5
44	971	1000	97.1	2.9	16	1.6
45	984	1000	98.4	1.6	7	0.7
46	974	1000	97.4	2.6	14	1.4
47	979	1000	97.9	2.1	12	1.2
48	977	1000	97.7	2.3	10	1.0
49	973	1000	97.3	2.7	16	1.6
51	971	1000	97.1	2.9	19	1.9
52	983	1000	98.3	1.7	7	0.7
53	982	1000	98.2	1.8	7	0.7
54	979	1000	97.9	2.1	10	1.0
55	973	1000	97.3	2.7	13	1.3
56	980	1000	98.0	2.0	10	1.0
57	974	1000	97.4	2.6	13	1.3
58	957	1000	95.7	4.3	23	2.3
59	968	1000	96.8	3.2	15	1.5
61	971	1000	97.1	2.9	8	0.8
62	977	1000	97.7	2.3	14	1.4
63	970	1000	97.0	3.0	16	1.6
64	977	1000	97.7	2.3	13	1.3
65	983	1000	98.3	1.7	10	1.0
66	968	1000	96.8	3.2	18	1.8
67	963	1000	96.3	3.7	19	1.9
68	970	1000	97.0	3.0	11	1.1
69	961	1000	96.1	3.9	9	0.9
70	978	1000	97.8	2.2	19	1.9
72	985	1000	98.5	1.5	12	1.2
73	971	1000	97.1	2.9	20	2.0
74	975	1000	97.5	2.5	17	1.7
75	977	1000	97.7	2.3	12	1.2
76	973	1000	97.3	2.7	15	1.5
77	971	1000	97.1	2.9	11	1.1
78	971	1000	97.1	2.9	13	1.3
79	963	1000	96.3	3.7	17	1.7
80	969	1000	96.9	3.1	11	1.1
81	977	1000	97.7	2.3	14	1.4
82	987	1000	98.7	1.3	10	1.0
83	968	1000	96.8	3.2	16	1.6
84						
85	961	1000	96.1	3.9	21	2.1
86	980	1000	98.0	2.0	11	1.1
87	960	1000	96.0	4.0	16	1.6
88	966	1000	96.6	3.4	16	1.6
89	950	1000	95.0	5.0	17	1.7
90	972	1000	97.2	2.8	14	1.4
91	978	1000	97.8	2.2	16	1.6
93	983	1000	98.3	1.7	11	1.1
94	976	1000	97.6	2.4	16	1.6
95	974	1000	97.4	2.6	22	2.2
96	986	1000	98.6	1.4	9	0.9
97	971	1000	97.1	2.9	15	1.5
98	972	1000	97.2	2.8	21	2.1
99	975	1000	97.5	2.5	17	1.7
100	978	1000	97.8	2.2	11	1.1
Average	976.1	1000.0	97.6	2.4	12.9	1.3

Figure 2.2: On- and off-target bead count rates of individual bead regions pipetted into separate wells. The well containing Region 84 was not properly read by the Bio-Plex 200.

carryover refers to bead counts originating from beads in previously analyzed wells. It may be the consequence of beads adhering to the sample needle and being carried

over to the next well, or perhaps it is the result of beads from previously analyzed wells remaining in the microfluidic channels in the pathway to the detectors. The cause of systematic misclassification, on the other hand, is not precisely known to us. However, it is likely due to spectral overlap of a region's emission profile into that of another.

The bead count data was arranged into an 80 x 80 matrix listed by bead region number in ascending order on each axis (Figure 2.1). A 3-color scale was applied where green represents counts of 950 or greater, yellow represents counts between 2 and 25, and red represents a count of 1. Arranged in this manner, high bead counts should occur along the diagonal, corresponding to counts in regions matching the labeled regions. Every bead region was correctly identified according to its labeled region, as illustrated by the green diagonal in the figure. In addition, carryover from the previous well was always observed, illustrated as the yellow diagonal immediately below the green diagonal. Carryover was responsible for 1.3%, on average, of the total bead count in each well and accounted for 54% of the average off-target bead count rate (Figure 2.2). Data from a separate bead validation experiment were used to quantify the number of wells where carryover can be detected (Figure 2.3). Carryover was limited to just one well the majority of the time (64%), but it was also observed two (28%) or sometimes even three (8%) wells away.

Systematic misclassification appeared as an additional diagonal above the green diagonal (Figure 2.1). Bead counts were obtained 4 to 11 regions "above" the interrogated bead region (Figure 2.4). The "distance" peaked at 11 (up to Bead Region 80) and then shrank to 9 for Bead Regions 83-90. Bead Regions 70, 81, and 82 appeared to have no artefactual counts above their labeled region (Figure 2.4b). Bead Regions 91-100 also appeared to have no artefactual counts above their labeled region, but it is possible that the misclassified regions are above Bead Region 100. Since the Bio-Plex 200 is not compatible with bead regions above 100, misclassifications in regions above 100 would not be determined by this instrument. An analysis of Bead Regions 91-100 on the Bio-Plex 3D, which is compatible with up to 500 regions, would potentially reveal the regions of systematic misclassification that the Bio-Plex 200 could not.

Bead count method. The Bio-Plex 200 offers two methods for counting beads: per region and total classified. When the "per region" method is selected, the instrument will attempt to count a user-specified number of beads for each region defined in the protocol of the assay. The manufacturer recommends that at least

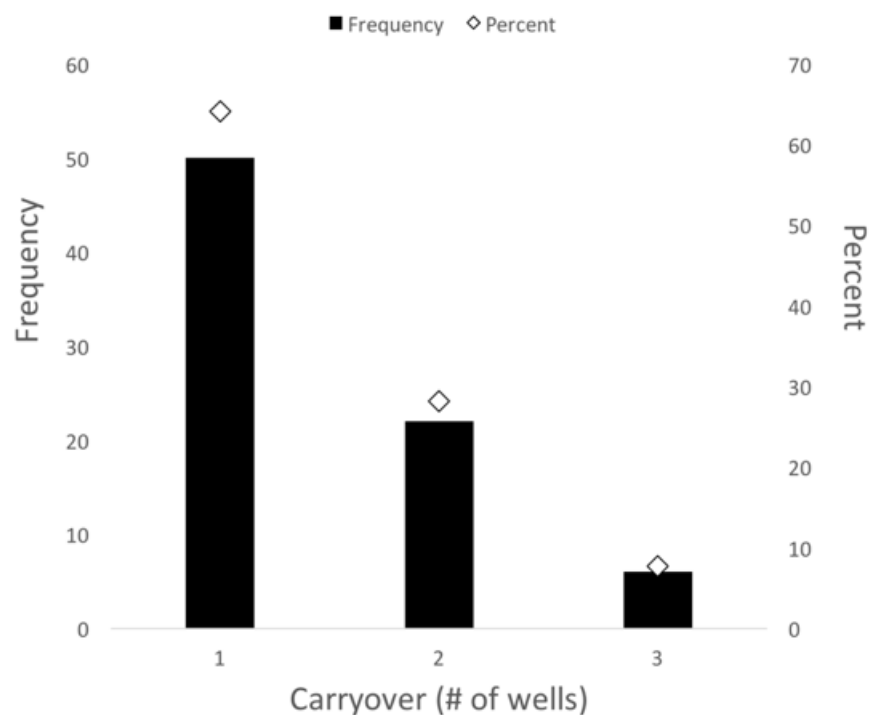
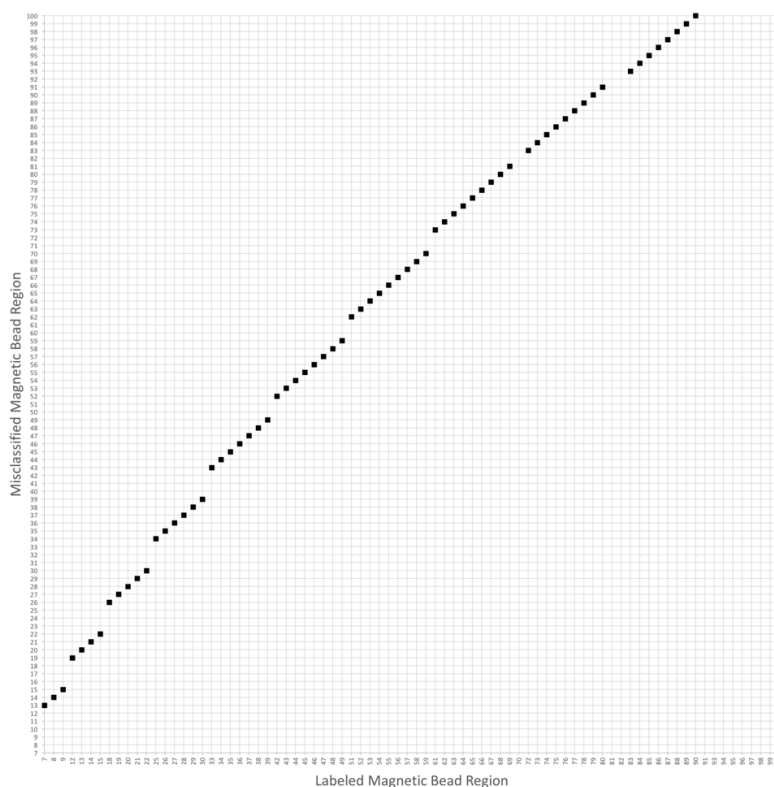


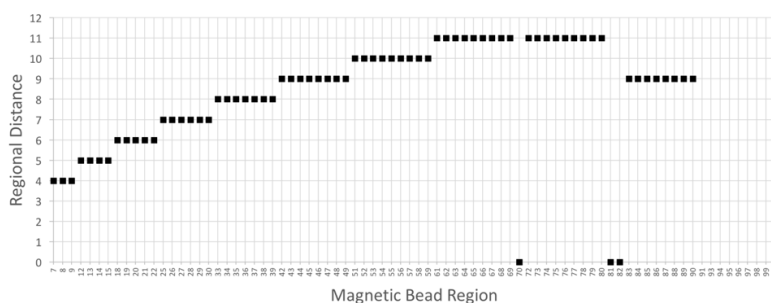
Figure 2.3: Quantification of bead carryover. Histogram depicting the frequency (left, bars) and percentage (right, diamonds) of the number of wells in which bead carryover was detected.

50 beads be counted per region in each well for statistically robust measurements. Once the machine has counted the user-specified number of beads for each region, it will move on to the next sample. However, bead counts in regions that exceed the user-specified number, along with their fluorescence intensity values, are included in the final data set. The “total classified” method instructs the machine to count a user-specified number of beads total, across all protocol-defined regions, for each well. The machine simply counts the total number of beads and will proceed to the next well after counting the user-specified number of beads per well.

If a bead mixture of n -plex consists of an equal concentration of beads of each region, then $P = \frac{T}{n}$, where T is total bead count and P is per region bead count. Commercial bead mixtures are typically prepared so that all bead regions are present in equal concentrations. For these mixtures, the two read methods will produce similar bead counts, as long as the formula above is obeyed. However, custom bead mixtures may not always be composed of an equal concentration of each region, owing to the numerous washing and pipetting steps involved during the coupling procedure. For this reason, the “total classified” method may provide a user with greater flexibility



(a) Graph depicting misclassified magnetic bead region as a function of labeled magnetic bead region. Gaps in the x -axis at Bead Regions 70, 81, and 82 indicate that these regions do not have a systematically misclassified bead region. Misclassifications for labeled Bead Regions 91-100 are not shown because the Bio-Plex 200 cannot classify regions above 100.



(b) Graph depicting distance to most commonly misclassified region as a function of labeled magnetic bead region. Distance reflects only the Bio-Plex 200-compatible magnetic bead region set. Distance ranges from 4 to 11 “above” the labeled magnetic bead region. A regional distance of 0 at Bead Regions 70, 81, and 82 indicates that these regions do not have a systematically misclassified bead region.

Figure 2.4: Systematic misclassification of magnetic bead regions. Both graphs show only the compatible magnetic bead regions for the Bio-Plex 200 on the x -axis.

and can increase efficiency by avoiding the extra processing time required to count underrepresented bead regions. Another benefit of the “total classified” counting strategy is that multiple bead mixtures composed of different bead regions can be processed using the same protocol in a single run.

Median Fluorescence Intensity (MFI). The Bio-Plex 200 utilizes a phycoerythrin fluorescent reporter to determine the result of an assay. Interestingly, the value reported is the median of the fluorescence intensity of the beads counted in a particular region. The selection of the median as the reported value of the signal was likely driven by the fact that outliers minimally affect the median of a data set, but can have a substantial impact on the mean of the same data set. Given that up to 4% of the beads counted in a particular well may originate from another well, reporting the median fluorescence intensity is a simple, yet effective, method of ensuring that the value accurately reflects the condition of the beads in the interrogated well.

By default, the fluorescence intensity value of individual beads is not disclosed to the user. However, it is possible to obtain these data by modifying the Document Export Properties within the Bio-Plex Manager Software settings.

Data acquisition on the Bio-Plex 200. Users can select pre-defined panels corresponding to commercial bead kits or define custom sets in the Analytes section of the pre-run setup. However, these settings only determine the regions that will be displayed during a run and exported to Excel after a run. In reality, the Bio-Plex 200 collects data from all compatible bead regions during a run. Therefore, a user can open the RBX data file of a previous run, re-define the panel of regions in the run settings, and re-export the data. This is particularly useful if a region was excluded by mistake, as it allows data to be recovered from potentially depleted samples without having to repeat a run.

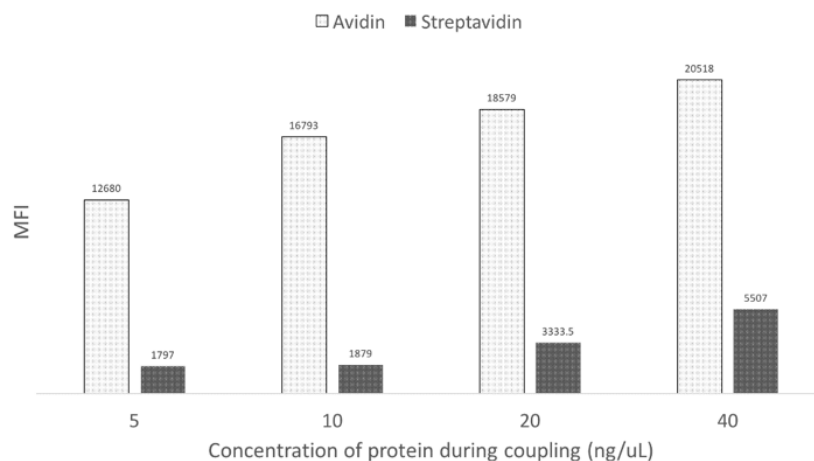
Scaling down the coupling protocol. The manufacturer’s bead coupling protocol instructs users to apply 5-12 μg of protein to couple 1.25×10^6 beads in a total volume of 500 μL at 1x scale. These values translate to three different quantities to control during coupling – mass of protein per bead (4-9.6 pg/bead), protein concentration (10-24 ng/ μL), and number of beads per unit volume (2,500 beads/ μL). The number of beads per unit volume is not likely to be an important factor for coupling since the beads comprise only 0.036% of the total volume of the reaction. Therefore, we sought to determine which of the two remaining quantities were the primary determinant of efficient coupling, especially when coupling fewer beads. To address this question, 1.25×10^4 beads were coupled to avidin or streptavidin at either 4

pg/bead or 10 ng/ μ L in a total volume of 500 μ L. Biotinylated goat IgG at 2 ng/ μ L was then added to the avidin- and streptavidin-coupled beads. The beads were pooled, stained with 1x streptavidin-phycoerythrin, and processed on the Bio-Plex. The results showed that protein concentration, not mass of protein per bead, was the key parameter to control for efficient coupling (data not shown).

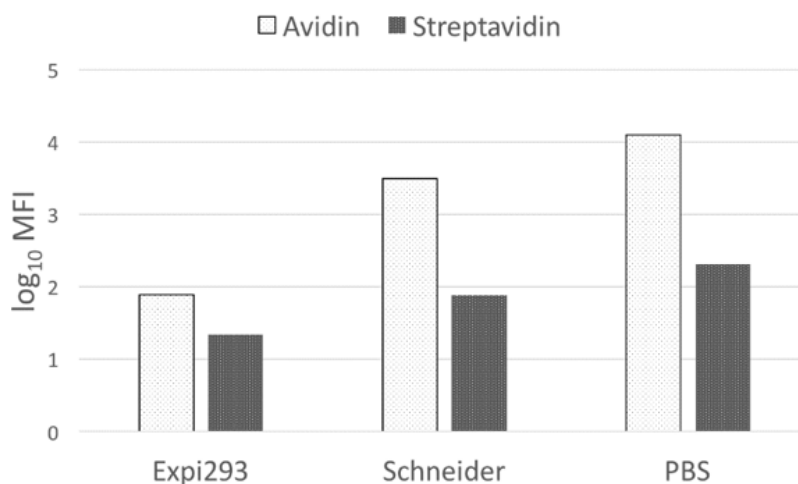
Coupling capture proteins. The magnetic Bio-Plex beads are functionalized with carboxyl groups on their surface. Carbodiimide crosslinker chemistry is employed in a 2-step reaction to render them suitable for amine coupling. The carboxyl group reacts with EDC to form an O-acylisourea intermediate, which is followed by reaction with S-NHS to form an amine-reactive sulfo-NHS ester. The ester can then react with primary amines of proteins or amine-modified oligonucleotides to form an amide bond, covalently linking them to the bead surface. The ability of a researcher to choose which reagents to couple forms the essence of custom bead-array assays. However, coupling is irreversible and a bead is committed to its reagent thereafter.

One way to enhance the versatility of the beads is to couple them to avidin, streptavidin, or Protein A, which can capture biotinylated or Fc-fusion biomolecules. Avidin and streptavidin were coupled to magnetic Bio-Plex beads at four different concentrations and tested for their ability to bind biotinylated IgG in PBS. Avidin outperformed streptavidin at every concentration (Figure 2.5a). The ability of the avidin- or streptavidin-coupled beads to bind biotinylated IgG in conditioned cell culture media was also investigated. Avidin-coupled beads were able to more effectively bind biotinylated IgG than streptavidin-coupled beads in all three media (Figure 2.5b). The amount of binding of biotinylated IgG to the coupled beads was inversely proportional to the amount of biotin in the cell culture media. Expi293 media, with a biotin concentration of 1.46 mg/L (D. Judd, personal communication), was the least suitable media for binding to beads. The PBS used in this experiment contained no biotin, and it was the optimal buffer for biotinylated IgG binding to beads. Schneider cell medium has a reported biotin concentration of 0 mg/L (D. Judd, personal communication), but binding was not as efficient as it was with PBS. Other factors present in the conditioned medium may interfere with binding, or it is possible that Schneider cells release biotin into the medium during culture. These results indicate that biotin concentration should be considered when binding biotinylated proteins to avidin- or streptavidin-coupled beads from cell culture supernatants.

The IgG Fc domain is a popular fusion tag for overexpression of proteins in cell



(a) Avidin and streptavidin were coupled to magnetic Bio-Plex beads at four different concentrations ranging from 5 to 40 ng/μL, incubated with biotinylated IgG, and then stained with streptavidin-phycoerythrin. Avidin produced higher MFI than streptavidin at every coupling concentration.



(b) Avidin was more effective than streptavidin at binding biotinylated IgG in cell culture media. The efficiency of capture of biotinylated proteins onto avidin- or streptavidin-coupled beads is dependent on the concentration of biotin in solution.

Figure 2.5: Comparison of avidin and streptavidin as bead-coupled capture reagents for biotinylated proteins. MFI = median fluorescence intensity.

culture. Its ability to enhance expression and solubility of its fusion partner has been well-documented. We therefore sought to examine if Protein A-coupled beads could effectively bind IgGs and Fc-fusion proteins in solution. However, an additional concern that we needed to evaluate was whether a bead-bound IgG or Fc-fusion protein could “jump” to a bead of a different region identity in a multiplexed assay,

a process we referred to as “bait jumping.” Bait jumping would be a fundamental design flaw that would eliminate Protein A as a useful capture reagent in these assays.

Protein A was coupled to five different bead regions, and biotinylated human IgG was loaded onto a fraction of beads of each region. Non-biotinylated human IgG was loaded onto the remainder of beads of each region. Five different bead pools were created by mixing one biotinylated human IgG-loaded bead region with four non-biotinylated human IgG-loaded bead regions (Figure 2.6a). The bead pools were incubated at 4 °C and evaluated at five different time points by staining with streptavidin-phycoerythrin. The results indicated that Protein A was able to bind IgG and that bait jumping was not observed for any of the bead pools up to 34 days after mixing (Figure 2.6b).

The Protein A-coupled, IgG-loaded beads were then subjected to a variety of harsh conditions to investigate their stability and to explore the limitations of Protein A capture (Figure 2.7). The beads were subjected to one or two of the following conditions: boiling, low pH, incubation with competitor, and incubation in conditioned cell culture media. The results and their interpretation are shown in Figure 2.7b. Beads were subjected to pH 3 for 5 minutes, neutralized to pH 7, and then incubated for an additional 30 minutes at room temperature to allow ample time for re-binding of the eluted IgG to the Protein A-coupled beads. Interestingly, no re-binding was observed. We reasoned that the femtomolar concentration of the eluted IgG combined with a binding equilibrium favoring an unbound state resulted in the lack of re-binding. However, when beads were subjected to pH 3 and then incubated with a chemically-biotinylated human IgG at ~67 nM, a high signal was observed in all bead regions, indicating that Protein A was capable of re-binding IgG after pH 3 treatment.

When Protein A-coupled, IgG-loaded beads were incubated with a competitor for Protein A binding sites, an increased signal was observed in all bead regions. Both competitors tested, a monobiotinylated mCherry-Fc and a chemically-biotinylated human IgG, produced similar results, indicating that proteins captured via bead-bound Protein A can be exchanged when a competitor is present at a sufficient concentration. Chemically-biotinylated IgG produced higher signals in every bead region when the beads were first subjected to pH 3 followed by incubation with the competitor, suggesting that only partial exchange occurred when competitors were added without pH 3 treatment. Lastly, PBS at pH 6.5 and conditioned cell

	Region 28	Region 29	Region 33	Region 34	Region 37
Mix 1	biotinylated human IgG	human IgG	human IgG	human IgG	human IgG
Mix 2	human IgG	biotinylated human IgG	human IgG	human IgG	human IgG
Mix 3	human IgG	human IgG	biotinylated human IgG	human IgG	human IgG
Mix 4	human IgG	human IgG	human IgG	biotinylated human IgG	human IgG
Mix 5	human IgG	human IgG	human IgG	human IgG	biotinylated human IgG

(a) Bait-capture map of five bead mixes used in the study.

Key:

		Region 28	Region 29	Region 33	Region 34	Region 37
Day 0	Mix 1	5932	16	23	30	17
	Mix 2	11	7426	22	19	16
	Mix 3	12	16	7293	21	15
	Mix 4	13	19	26	7919	18
	Mix 5	13	18	24	25	11249
Day 1	Mix 1	7670	20	28	30	22
	Mix 2	15	9531	29	28	21
	Mix 3	14	19	9769	27	21
	Mix 4	20	27	34	10313	31
	Mix 5	17	26	35	37	11149
Day 3	Mix 1	8653	33	42	49	39
	Mix 2	19	10857	35	36	34
	Mix 3	20	29	10900	38	34
	Mix 4	37	54	68	12138	71
	Mix 5	27	40	46	59	16588
Day 5	Mix 1	7541	36	45	59	42
	Mix 2	22	9941	41	44	42
	Mix 3	24	34	9373	47	47
	Mix 4	42.5	59	72	10814.5	83
	Mix 5	31	44	56	71	15307
Day 12	Mix 1	7735	52	65	86	63
	Mix 2	36	9579	64	74	73
	Mix 3	38	56	9754	79	80
	Mix 4	71	102	110	11272	149
	Mix 5	56	79	97	123	16147
Day 34	Mix 1	6314	59.5	88.5	85	71
	Mix 2	229	7411	91	141	201.5
	Mix 3					
	Mix 4					
	Mix 5					

(b) The five bead mixes were incubated for the indicated time points, stained with streptavidin-phycoerythrin, and processed on the Bio-Plex 200. MFI values were obtained and a 2-color scale was applied to the data, where green represents high MFI values and white represents low MFI values. MFIs reflect a step-ladder pattern corresponding to the bait-capture map, suggesting that “bait jumping” is not occurring at a detectable level up to 34 days after mixing. (Note: On Day 34, only two bead mixes were analyzed.)

Figure 2.6: Investigation of “bait jumping” on Protein A-coupled magnetic Bio-Plex beads. MFI = median fluorescence intensity.

	Region 28	Region 29
Mix 1	biotinylated human IgG	human IgG
Mix 2	human IgG	biotinylated human IgG

(a) Map of bead mixes used in the study.



Condition		Region 28	Region 29	Region 33	Region 34	Region 37	Interpretation
1x PBS	Mix 1	6314	59.5	88.5	85	71	Biotinylated IgG did not jump onto other ProA-coupled, IgG-loaded bead regions.
	Mix 2	229	7411	91	141	201.5	
Boiled for 5 minutes	Mix 1	731	26	16.5	35	33	Boiling caused IgG to fall off of ProA-coupled beads, but it did not re-bind to beads.
	Mix 2	9	834.5	16	28	18	
pH 3 for 5 minutes then neutralized to pH 7	Mix 1	1026	128	106	89	151	Low pH caused IgG to elute off of ProA-coupled beads, but eluted IgG did not re-bind to beads.
	Mix 2	30	1302.5	40	36	38	
pH 3 for 30 minutes then neutralized to pH 7	Mix 1	943	38.5	30	26	33	Same as pH 3 for 5 minutes. Extended exposure to pH 3 had no effect.
	Mix 2	21	1212	29.5	31	39	
pH 6.5	Mix 1	5707.5	50.5	65	77	63	ProA-coupled, IgG-loaded beads can withstand slightly acidic conditions, like overgrown cell culture media.
	Mix 2	41.5	6932	64.5	76	99	
monobiotinylated mCherry-Fc (100 ng/uL)	Mix 1	5954	1524.5	1602.5	1695	1703.5	Signal increased in all bead regions, indicating that exchange can occur between ProA-bound IgG and solution Fc-fusion.
	Mix 2	2987.5	7330	2020	1856	2168.5	
biotinylated human IgG (10 ng/uL)	Mix 1	9751	3540	3191	3506	4887	Signal increased in all bead regions, indicating that exchange can occur between ProA-bound IgG and solution IgG.
	Mix 2	2720	13270	2548	3947.5	4813	
pH 3 for 5 minutes then biotinylated human IgG (10 ng/uL)	Mix 1	22202	21582	20421	20957.5	24322	ProA-coupled beads are capable of re-binding solution IgG after pH 3 exposure, provided solution IgG is sufficiently concentrated.
	Mix 2	17269.5	23770	19896	19827	23658.5	
conditioned Expi293 supernatant	Mix 1	5721	50	69	76	63	Biotinylated IgG did not jump onto other ProA-coupled, IgG-loaded bead regions.
	Mix 2	45	7428.5	72	83.5	101.5	
conditioned S2 supernatant	Mix 1	4270.5	45	63	61	59	Biotinylated IgG did not jump onto other ProA-coupled, IgG-loaded bead regions.
	Mix 2	38	6232	77	66	78	
no StrepPE (negative control)	Mix 1	9	12	17	11	10	Beads have an auto-fluorescence of roughly 10-20 fluorescence units.
	Mix 2	9	10	19	10	11	

(b) The bead mixes were subjected to the stated conditions, stained with StrepPE, and processed on the Bio-Plex 200. MFI values were obtained and a 2-color scale was applied to the data, where green represents high MFI values and white represents low MFI values.

Figure 2.7: Stability of Protein A-coupled beads loaded with biotinylated bait in various conditions. MFI = median fluorescence intensity.

culture media from Schneider and Expi293 cells did not cause bait jumping nor did it significantly reduce signal in the biotinylated IgG-loaded bead region. Taken together, these data reveal that Protein A is a robust capture protein compatible with multiplexed bead-based assays.

*Chapter 3***HIGH-THROUGHPUT MONOCLONAL ANTIBODY
PRODUCTION****3.1 Background**

Monoclonal antibodies (mAbs) have become an invaluable resource in molecular biology. They are the crux of many experimental techniques, including, but not limited to, immunohistochemistry (Coons, Creech, and Jones, 1941). Western blotting (Burnette, 1981; Towbin, Staehelin, and Gordon, 1979), fluorescence-activated flow cytometry (Leonore A. Herzenberg, De Rosa, and Leonard A. Herzenberg, 2000), chromatin immunoprecipitation (Gilmour and Lis, 1984; ENCODE Project Consortium et al., 2012; Gasper et al., 2014), and enzyme-linked immunosorbent assay (Engvall and Perlmann, 1971). They have also been recognized as powerful therapeutics against cancer (Hudziak et al., 1989; Maloney et al., 1997), HIV (Klein et al., 2012; Scheid et al., 2016), autoimmune disorders (Siegel et al., 1995), and a variety of other diseases. Their potential to prevent disease via vectored immunoprophylaxis is another area in which researchers are harnessing the power of mAbs (Balazs, J. Chen, et al., 2012; Balazs, J. D. Bloom, et al., 2013).

Prior to the ubiquity of monoclonal antibodies, serum from immunized animals was the primary antibody source for biological experiments. However, there are significant drawbacks associated with serum's usage as an antibody source. Serum is a complex matrix containing antibodies derived from many genetically diverse B cells and is therefore polyclonal. Each immunized animal displays a unique immune response profile, even after controlling for variables such as species and strain, adjuvant formulation, and immunization schedule, hence the antibody composition differs for each immunized animal. As a consequence, commercial entities that produce polyclonal antibodies tend to pool sera from many animals to increase the volume of sample defining a particular batch while minimizing the number of batches that must be assayed for potency and quality. Recommended working concentrations of polyclonal antibody sources are given as titers or dilution factors and vary depending on the batch, lot number, or production run as well as their intended application. Serum can be subjected to affinity chromatography (using Protein A, Protein G or antigen affinity chromatography), but the resulting purified

antibodies remain polyclonal.

Köhler and Milstein introduced a paradigm shift for production of antibodies through the advent of hybridoma technology in 1975 (Köhler and Milstein, 1975). The process begins by immunizing an animal (typically a mouse) with an antigen to generate B cells producing antibodies specific to the injected antigen *in vivo*. Primary B cells have a short lifespan and are thus refractory to cell culture. However, they can be harvested from an immunized animal and induced to fuse with immortal myeloma cells lacking a functional hypoxanthine-guanine phosphoribosyltransferase (HGPRT) to produce hybrid cells, also known as hybridomas. Following fusion, the cells are placed in selective hypoxanthine-aminopterin-thymidine (HAT) medium for 10-14 days. Aminopterin blocks *de novo* DNA synthesis pathways by inhibiting dihydrofolate reductase and forces cells to utilize nucleotide salvage pathways in order to survive. Unfused myeloma cells die in HAT medium because HGPRT is a critical enzyme in the purine salvage pathway of mammalian cells, whereas unfused primary B cells die because of their short lifespan. Hybridoma cells survive because they are immortal and express active HGPRT, enabling them to use hypoxanthine found in HAT medium in the purine salvage pathway. Most importantly, a subset of hybridomas secrete antibodies specific to the injected antigen. The final step of the procedure is dilution of the hybridomas into micro-well plates such that each well contains one cell. At this point, the antibodies secreted into the medium within each well are identical to each other, having the same primary structure and epitope recognition, because they are derived from a single parent cell (i.e. monoclonal).

This was a breakthrough achievement because it provided an infinitely renewable resource of monoclonal antibodies via permanent cell lines, overcoming the problems of heterogeneity and batch-to-batch variability presented by polyclonal antibodies. Even more remarkably, the discovery was made before the emergence of the Sanger method of DNA sequencing (Sanger, Nicklen, and Coulson, 1977) and polymerase chain reaction (PCR) (Saiki et al., 1985; Mullis and Faloona, 1987), two other technologies that would reshape the landscape of molecular biology. Köhler and Milstein were two of three recipients of the 1984 Nobel Prize in Physiology or Medicine for “the discovery of the principle for production of monoclonal antibodies.”

A considerable amount of effort has been devoted to the improvement of production of mAbs, given their indispensability in biology and medicine. In particular, scientists have focused on increasing throughput and reducing the amount of time between first injection and characterization of antibody. Broadly speaking, these efforts can

be divided into two categories: immunological and technical. Immunological considerations involve expanding the diversity of the immune response to include multiple target proteins, enhancing antigenicity of targets, increasing antigen- and isotype-specific antibody yield, optimizing immunization schedules, and exploring alternatives to hybridoma technology. On the other hand, technical concerns primarily revolve around screening methods. Typical hybridoma screens are time-sensitive and are conducted on thousands of clones using limited volumes of supernatant. Therefore, screening techniques that reduce labor or improve efficiency are highly desired.

3.2 Introduction

MAbs are routinely used in basic research and are increasingly being utilized in the clinic as therapeutics to treat a wide variety of conditions. Because demand for mAbs is rising, strategies for achieving high-throughput monoclonal antibody production have been discussed (Chambers, 2005; Chiarella and Fazio, 2008). Using conventional hybridoma technology, three approaches need to be combined to achieve this goal – multiplexed immunization, efficient screening methods, and automation.

Multiplexed immunization, in the context of vaccines, has been known for over a century as an effective immunization strategy (Castellani, 1913; Castellani, 1915). In the 1940s, reports on the safety and efficacy of combination vaccines against diphtheria and tetanus (Sauer and Tucker, 1942) or against diphtheria, tetanus, and pertussis (Hamilton, 1945) culminated in their U.S. FDA approval in 1947 and 1949, respectively. Given its long history in vaccinology, multiplexed immunization is a logical component of a high-throughput monoclonal antibody production workflow. In one study, a multiple-antigen, single fusion (MASF) approach produced a higher number of hybridomas than a single-antigen, pooled fusion (SAPF) approach (Chiarella, Leuener, et al., 2011), providing evidence that multiplexed immunization can be incorporated into a successful hybridoma-based mAb production pipeline.

Cell-based immunization and hybridoma screening have also been described in the literature. Indeed, Köhler and Milstein established hybridoma technology using sheep red blood cells as both an immunogen and a hybridoma screening reagent in a plaque assay technique (Köhler and Milstein, 1975). The use of a single cell line as both immunogen and screening reagent was later refined by replacing the plaque assay with a system using a *LacZ* reporter gene and generalized to include any target

protein that could be expressed and localized to the cell surface (Mesci and Carlyle, 2007; P. Chen, Mesci, and Carlyle, 2011). The majority of reports using cell-based immunogens utilize antigen-overexpressing cells xenogeneic or allogeneic to the host, but much of the immune response may be directed away from the antigen in this case (Dreyer et al., 2010; Ebersbach and Geisse, 2012). There is evidence in the literature that antigen-overexpressing cells syngeneic to the host may be sufficient to induce an immune response (Tokuyama, 1975).

Hybridoma supernatants are typically screened using ELISA against a single antigen. However, the limited volume of available supernatant makes screening against multiple antigens difficult. Microarrays have been presented as a solution to this problem. De Masi and colleagues spotted hybridoma supernatants onto antigen-coated glass slides and detected antigen-specific mouse antibodies with Cy3-conjugated anti-IgG and Cy5-conjugated anti-IgM in their antigen microarray assay (AMA) (De Masi et al., 2005). This assay design allowed IgG- and IgM- isotyping simultaneously with antigen-specificity screening, but cross-reactive antibodies could only be identified comparing signal across different antigen-coated slides. By arraying antigens instead of hybridomas, cross-reactivity and specificity were assessed simultaneously (Yu et al., 2010; Staudt, Müller-Sienerth, and Wright, 2014).

We created Balb/c 3T3 stable cell lines expressing antigen on the cell surface and then injected pools of up to 14 lines into female Balb/c 3T3 mice. Then, we used two semi-automated methods for hybridoma screening. The first method was a pooled-antigen ELISA screen, and the second method was a multiplexed bead-based screen capable of simultaneously determine antibody specificity, cross-reactivity, and isotype.

3.3 Materials and Methods

Plasmid construction. Extracellular domain genes were PCR-amplified and cloned into the pCR8 entry vector using the pCR8/GW/TOPO TA Cloning® Kit (Life Technologies Cat. K2500-20) according to the manufacturer's protocol. Entry vectors containing extracellular domain genes in the proper orientation were then converted into expression vectors using a modified destination vector and the Gateway® LR Clonase™ II Enzyme Mix (Life Technologies Cat. 11791-020) in a Gateway LR reaction. For stable cell line production, the destination vector was a modified Gateway® pcDNA-DEST40 plasmid containing a PGK promoter, HGH signal peptide sequence, and sequence encoding the mouse CD8 α transmembrane

and cytoplasmic domains. The cytoplasmic domain of mouse CD8 α was truncated to eliminate potential downstream signaling through the CD8 receptor. For soluble antigen production, the destination vector was a modified pMT/BiP/V5-His plasmid (Invitrogen Cat. V4130-20) containing a Gateway recombination cassette, HRV 3C protease site, and Fc tag from human IgG1 between the BiP signal sequence and the C-terminal V5 epitope.

Stable cell lines. Balb/c 3T3 fibroblasts (ATCC® CCL-163™) were grown to ~70% confluence in 6-well plates in Dulbecco's Modified Eagle's Medium (DMEM) (Life Technologies Cat. 12800-017) supplemented with 10% (v/v) bovine calf serum (ATCC® Cat. 30-2030). They were then transfected with 4 μ g of plasmid DNA and 8 μ g of Lipofectamine 2000 (L2K) (Life Technologies). After 24 hours, the cells were passaged 1:10 and Geneticin (Life Technologies Cat. 10131-027) was added to 400 ng/ μ L final concentration. Cells were maintained in 400 ng/ μ L Geneticin thereafter.

Secreted antigen expression. Schneider 2 (S2) cells were transiently transfected with plasmids encoding secreted antigen-human IgG1 Fc fusion proteins using Effectene (Qiagen) according to the manufacturer's protocol. CuSO₄ was added to 1 mM final concentration 24 hours after transfection. Supernatants were harvested after 4 days and stored at 4 °C.

Flow cytometry. Adherent stable cell lines were detached from tissue culture wells with Accutase (Innovative Cell Technologies Cat. AT104-500), washed twice with 1x PBS, and resuspended in flow cytometry buffer (1x HBSS, 2.5 μ g/ μ L BSA, 5 mM Mg²⁺, 10 mM HEPES, and 50 ng/ μ L DNase I). The cells were then stained with Anti-Mouse CD8 α PE (eBioscience Cat. 12-0081) using 0.2 μ g of antibody per 100 μ L of cell suspension. After incubating on ice for 30 minutes, the cells were washed three times with flow cytometry buffer, resuspended in 500 μ L of flow cytometry buffer, and analyzed on a flow cytometer.

Mice immunizations and sera screening. Female Balb/c mice aged 4-6 weeks (Charles River) were injected intraperitoneally with 10⁶ to 10⁷ live cells in 300 μ L of PBS per injection. Primary and secondary boosts were accompanied by injection of Sigma Adjuvant System® (Sigma-Aldrich Cat. S6322) at a different site to preserve the integrity of the cells. Blood was extracted from the tail vein 1 week post injection, allowed to clot, and spun at 20,000 x g for 30 minutes at room temperature. The serum supernatant was then diluted 1:5,000 in 5% (w/v) BSA blocking buffer and used as primary antibody in Western blot analysis against 100

ng of soluble versions of the injected antigens. The serum with the highest titer while showing the broadest response was identified and the spleen of the corresponding mouse was harvested according to approved animal protocols.

Hybridoma production. Splenocytes from immunized mice were mixed with Ventrax HL-1™ Friendly Myeloma-653 cells at a ratio of 10 splenocytes to 1 myeloma cell and induced to fuse with PEG. The cells were then subjected to selection in HAT medium for 10-14 days. Following selection, the hybridomas were serially diluted and plated onto 96-well plates. Wells were examined under a bright-field microscope to ensure that they contained a single cell. Supernatants were collected after 1 week and screened by ELISA or Bio-Plex. Hybridomas of interest were subcloned and rescreened 1 week later.

Hybridoma screening: semi-automated ELISA. A Tecan Evo 2 liquid handler was used for semi-automated ELISA screening of hybridoma supernatants. The assay protocol was divided into 5 robotic operations: 1) coating with capture antibody, 2) blocking, 3) antigen-immobilization, 4) hybridoma supernatant addition, 5) enzyme-linked detection antibody addition, and 6) substrate addition followed by plate read. 384-well plates (Nunc Cat. 460518) were coated overnight with 20 μ L of goat anti-human IgG (Fc γ specific) (Jackson ImmunoResearch Laboratories Cat. 109-005-098) at 10 ng/ μ L in 100 mM NaHCO₃ pH 9.6 buffer. The wells were then aspirated and blocked with 5% (w/v) BSA for 30-60 minutes at room temperature. The blocking buffer was removed and 20 μ L of S2 supernatants containing pools of up to 4 antigen-human IgG1 Fc fusion proteins were added to the wells. The plates were incubated at room temperature in a humidified chamber for 5-6 hours. After antigen immobilization, the wells were washed three times with 100 μ L of TBST followed by addition of 20 μ L of hybridoma supernatant to each well. The plates were incubated overnight at room temperature in a humidified chamber. The plates were then washed three times with TBST followed by the addition of 20 μ L of peroxidase-conjugated goat anti-mouse IgG (H+L) (Jackson ImmunoResearch Laboratories Cat. 115-035-003) diluted 1:40,000 in BSA blocking buffer. The plates were incubated for 3 hours at room temperature, washed three times with TBST, and 20 μ L of SuperSignal™ ELISA Femto Substrate (ThermoFisher Scientific Cat. 37075) was added to each well. Chemiluminescence at 425 nm was measured in a plate reader immediately after addition of substrate.

Hybridoma screening: semi-automated Bio-Plex. A Tecan Evo 2 liquid handler was used for semi-automated Bio-Plex screening of hybridoma supernatants. The

assay protocol was divided into 5 robotic operations: 1) hybridoma supernatant plate transfer, 2) addition of antigen-coupled, pooled, and blocked bead mixture to hybridoma supernatants, 3) biotinylated anti-mouse antibody addition, and 4) streptavidin-phycoerythrin addition followed by plate read. Antigen-human IgG1 Fc fusion proteins, CD8-hFc, and bovine IgG were purified from S2 cell supernatants using Protein A agarose resin (Pierce Cat. 20334). BSA (Pierce Cat. 23208) and anti-isotype antibodies (Rockland™ Antibodies and Assays goat anti-Mouse IgM Cat. 610-1107, Jackson ImmunoResearch Laboratories donkey anti-Mouse IgG Cat. 715-005-150, goat anti-Mouse IgM Cat. 115-005-075, goat anti-Mouse IgG Cat. 115-005-164) were purchased from commercial vendors. Protein A-purified tdTomato-hFc, human Fc and human IgG were obtained as gifts from J. Keeffe (Björkman lab). Baculovirus was obtained as a gift from the Caltech Protein Expression Center. GFP-MBP was expressed in *E. coli* and purified using amylose resin (New England BioLabs Cat. E8022). Proteins were buffer exchanged into PBS using desalting columns (ThermoFisher Cat. 89883), and total concentration was determined using a Bradford protein assay (Bio-Rad Laboratories Cat. 500-0006) using pre-diluted BSA standards (Pierce Cat. 23208). Approximately 320,000 Bio-Plex Pro Magnetic COOH beads of each region were coupled to 3.1 µg of protein according to the manufacturer's protocol. Coupled beads were counted and pooled such that the resulting multiplexed bead mixture had an equal number of beads of each region. The multiplexed bead set was diluted to a concentration of approximately 60 beads per region per µL and 5 µL was added to 50 µL of each hybridoma supernatant in low-profile 96-well PCR plates (Bio-Rad Laboratories Cat. HSP9631). The beads were allowed to incubate for 30 minutes at room temperature and then the plates were transferred to a 96-well ring-magnetic plate for 2 minutes. The supernatants were carefully aspirated and the plates were removed from the magnetic plate before the addition of 100 µL of PBST to each well. This process was repeated two more times and then 50 µL of biotinylated goat anti-mouse IgG (H+L) (Vector Laboratories Cat. BA-9200) at 2 ng/µL in 5% BSA blocking buffer was added to each well. After an incubation time of 30 minutes at room temperature, the plates were washed three times with PBST and then 1x SAPE, prepared from 100x stock (Bio-Rad Laboratories Cat. 171-304501) diluted in PBS, was added to each well. The beads were washed three times with PBST, resuspended in 50 µL of PBS, and analyzed on the Bio-Plex 200 instrument.

Data analysis. Raw data from the Bio-Plex runs were exported as Microsoft Excel worksheets and all subsequent analyses were performed in Excel. For initial screens,

three criteria were used to identify hits: median fluorescence intensity (MFI) threshold, signal-to-noise ratio (SNR), and monoclonality ratio (MR). SNR was calculated by dividing the MFI of each bead region in a hybridoma well by the MFI of the corresponding region in a PBS well. MR was calculated by dividing the MFI of each antigen in a hybridoma well by the maximum MFI of the other antigens in the same well. The precise values of the three criteria varied from plate to plate, and hits were identified as hybridomas exceeding any one of the three criteria. Elite hits met the following criteria: MFI threshold $>10^4$, SNR > 100 , and MR > 50 .

Amino acid sequence alignment. Extracellular domain sequences of human EPHA2, human EPHA3, human EPHA4, and murine EPHA2 were obtained from UniProtKB accession numbers P29317, P29320, P54764, and Q03145, respectively. Sequence alignment was performed using Clustal Omega.

3.4 Results

Trial 1: human/fly mix (14 antigens). Fourteen Balb/c 3T3 stable cell lines were created (Figure 3.1). Seven cell lines expressed human receptor tyrosine kinase extracellular domains, and the other seven lines expressed *Drosophila melanogaster* extracellular domains from the immunoglobulin superfamily (IgSF), leucine-rich repeat (LRR), and fibronectin type III (FnIII) families. Surface expression was confirmed by staining cells with a fluorescent anti-mouse CD8 α antibody in non-permeabilizing conditions followed by flow cytometry analysis (data not shown). The fruit fly antigen-expressing lines were pooled and fluorescence-activated cell sorting (FACS) was performed on the mixed line. The human antigen-expressing lines were analyzed individually by flow cytometry, and a mixed population was created by adjusting the proportion of each line to obtain an equal number of CD8 $^+$ cells of each line. The mixed human and fly cell lines were frozen in aliquots after mixing. Prior to injection, cells were thawed, passaged once or twice, and detached using Accutase. They were then washed twice with PBS and 10^7 cells were injected into the peritoneum of female Balb/c mice. Mice were injected a total of 5 times over a period of 6 months. The spleen of the mouse within the cohort with the highest antibody titer, as determined by Western blotting using sera obtained from the immunized mice, was then extracted and used for hybridoma production.

A total of 1,320 hybridoma supernatants were screened by ELISA. Due to the limited volume of hybridoma supernatant available for screening, antigens could not be screened individually. Instead, antigens were pooled into four bins, with each

Number	Protein/Annotation ID	Species
1	AXL	<i>H. Sapiens</i>
2	DDR1	<i>H. Sapiens</i>
3	EPHA2	<i>H. Sapiens</i>
4	EPHA3	<i>H. Sapiens</i>
5	EPHA4	<i>H. Sapiens</i>
6	ERBB3	<i>H. Sapiens</i>
7	TYRO3	<i>H. Sapiens</i>
8	CG1504	<i>D. Melanogaster</i>
9	CG4781	<i>D. Melanogaster</i>
10	CG7702	<i>D. Melanogaster</i>
11	Fish-lips (Fili)	<i>D. Melanogaster</i>
12	kekkon 5 (kek5)	<i>D. Melanogaster</i>
13	Toll-6	<i>D. Melanogaster</i>
14	windpipe (wdp)	<i>D. Melanogaster</i>

Figure 3.1: List of immunogens overexpressed on the surface of Balb/c 3T3 cell lines injected into female Balb/c 3T3 mice in Trial 1.

bin containing three or four antigens each (Figure 3.2). A total of 275 hybridoma clones were selected for rescreen: 118 clones secreted antibodies against the human antigens and 172 clones secreted antibodies against the fly antigens. (Data from the initial screen for the three clones that would eventually be selected are shown in Figure 3.3a.) Of the 275 clones selected for rescreen, 15 clones exhibited reactivity towards more than one antigen bin. The rescreen was performed the following day on 252 supernatants because 23 of the clones identified in the primary screen dropped out. A total of 57 unique clones were identified secreting antigen-specific antibodies (Figure 3.4), and 45 out of the 57 displayed the same specificity as in the primary screen, producing a correlation rate of 79% (data not shown). Three clones, each displaying reactivity toward unique antigen bins following rescreen of selected hybridoma supernatants from the initial screen (Figure 3.3b), were selected for subcloning: 3B7, 6F1 and 7E4.

The three hybridomas selected for subcloning produced a total of 78 unique clones for screening, of which 24 were visually confirmed as single cell. The supernatants of the subclones were screened by ELISA, and each supernatant was screened against the individual antigens in the bin to which specificity was previously ascribed. Hence, the deconvolution step necessitated by the antigen binning of the previous screens occurred at this time (Figure 3.5). A total of 11 subclones were identified

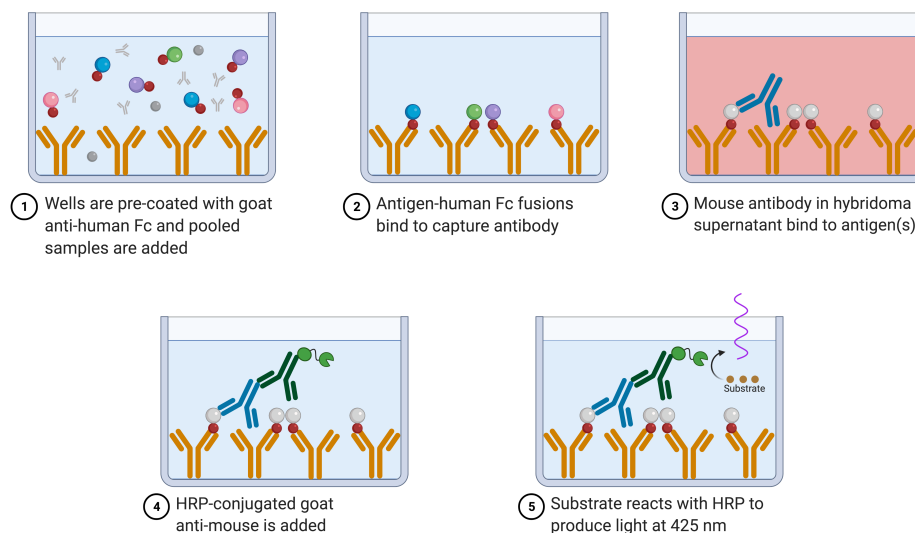


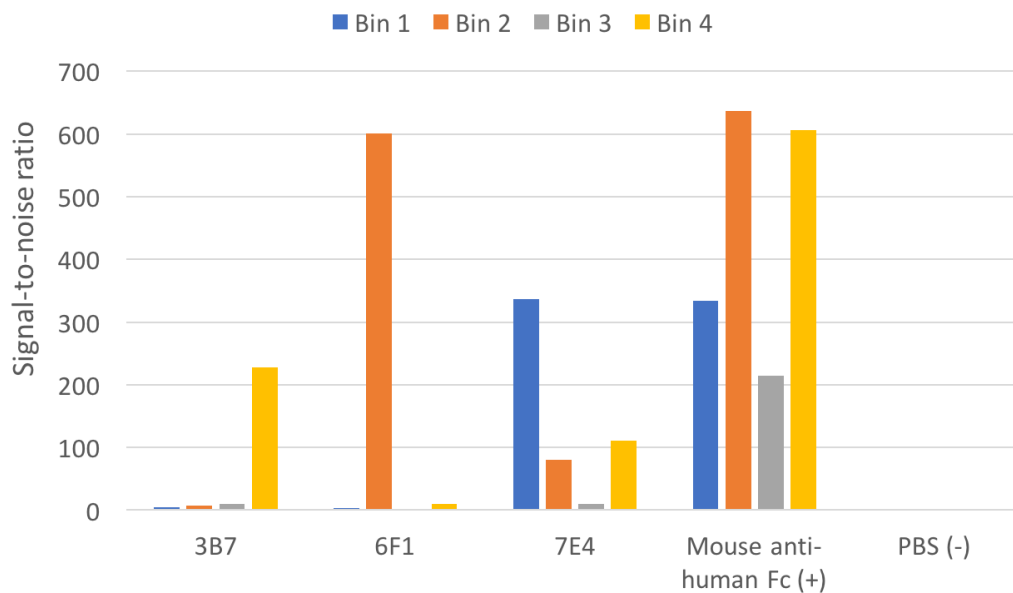
Figure 3.2: Hybridoma screening using pooled-antigen ELISA. Each well was loaded with up to 4 antigens. If mouse antibody (blue antibody in Steps 3, 4 and 5) binds to antigen, its specificity is not known until a deconvolution assay is performed. HRP = horseradish peroxidase. Created with BioRender.com

as hits – five from the 3B7 line, four from the 6F1 line, and two from the 7E4 line. Only one clone was identified as being both monoclonal and monospecific with high confidence: 3B7 B5. 3B7 B5 was identified as a mouse anti-windpipe antibody (Figure 3.6a). In addition to ELISA, 3B7 B5 was successfully used as a primary antibody in Western blotting (Figure 3.6b) and immunohistochemistry (IHC) applications (Figure 3.6c). IHC staining was performed on live-dissected stage 16 *D. melanogaster* embryos and the resulting staining patterns matched published windpipe expression patterns (Huff et al., 2002). The 3B7 B5 hybridoma line is now available through the Developmental Studies Hybridoma Bank under catalog number 3B7B5 and the antibody itself has an Antibody Registry ID of AB_2753229.

Interestingly, the four 6F1 subclones showed reactivity towards every antigen (Figure 3.6a). These results may indicate cross-reactivity due to shared epitopes between EPHA2, EPHA3, and EPHA4. However, they may also react to human Fc, as they also produced a signal against the CD8-hFc protein included as a control for non-specific binding.

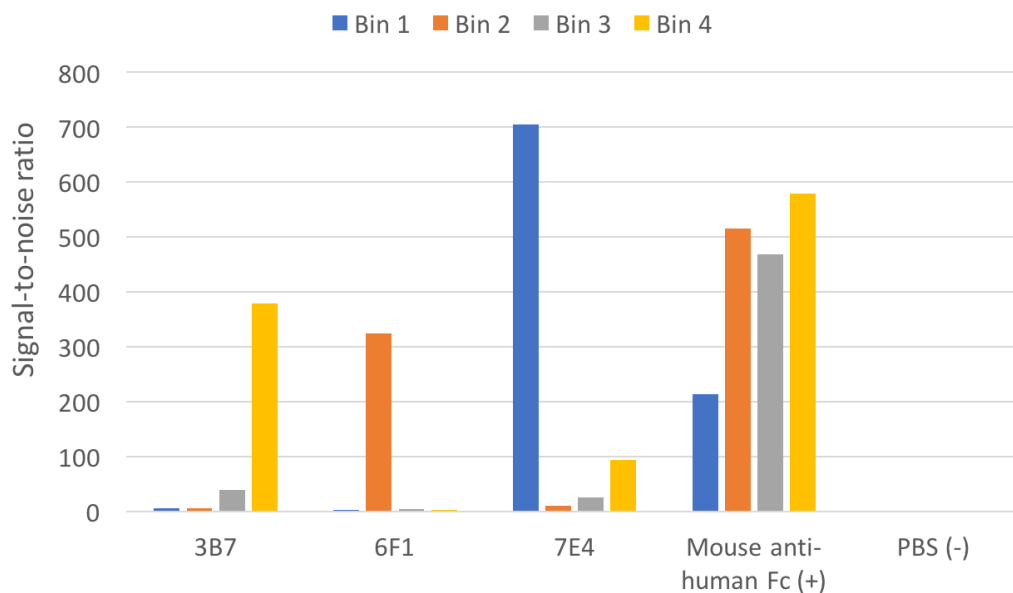
Trial 2: human mix (7 antigens). The mixed line of human antigen-expressing

Initial screen



(a) Results from initial screen.

Repeat screen



(b) Results from rescreen. Note how each hybridoma clone is specific to a different bin.

Figure 3.3: Signal-to-noise ratios of select clones in ELISA screen. Bin 1 is AXL, DDR1, ERBB3, and TYRO3. Bin 2 is EPHA2, EPHA3, and EPHA4. Bin 3 is CG1504, Fili, kek5, and Toll-6. Bin 4 is CG4781, CG7702, and wdp.

Initial Screen (Input: 1,320 clones)	Bin #	Antigens in Bin	# of hits	# of hits per species	Total # of hits	# reactive >1 bin	Total # unique clones	Hit Rate (%)
	Bin 1	AXL, DDR1, TYRO3, ERBB3	90	118	290	15	275	21
	Bin 2	EPHA2, EPHA3, EPHA4	28					
	Bin 3	CG1504, Fili, kek5, Toll-6	62	172				
	Bin 4	CG4781, CG7702, wdp	110					
Rescreen (Input: 252 clones)	Bin #	Antigens in Bin	# of hits	# of hits per species	Total # of hits	# reactive >1 bin	Total # unique clones	Hit Rate (%)
	Bin 1	AXL, DDR1, TYRO3, ERBB3	36	39	58	1	57	23
	Bin 2	EPHA2, EPHA3, EPHA4	3					
	Bin 3	CG1504, Fili, kek5, Toll-6	0	19				
	Bin 4	CG4781, CG7702, wdp	19					

Figure 3.4: Number of hits in hybridoma screen using pooled-antigen ELISA.

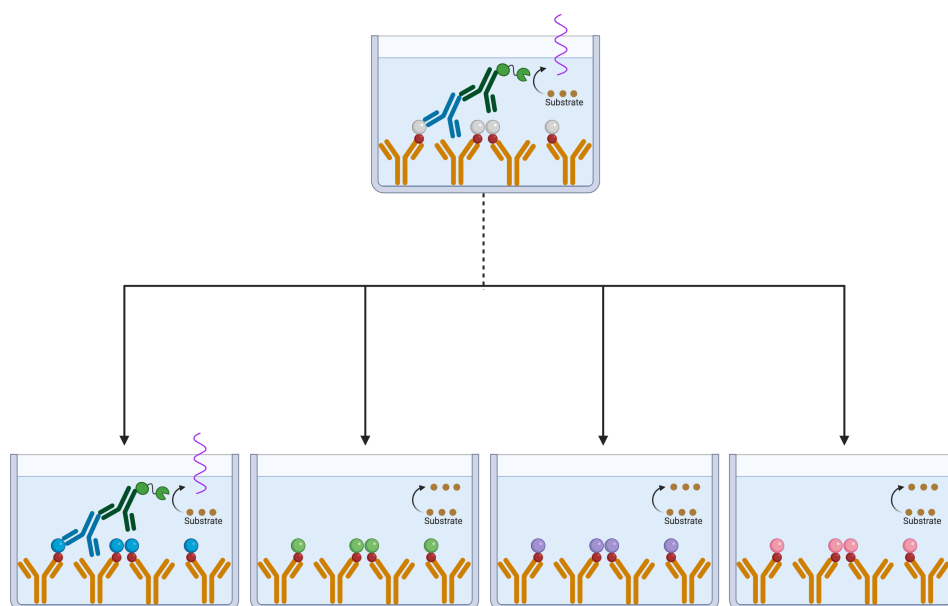
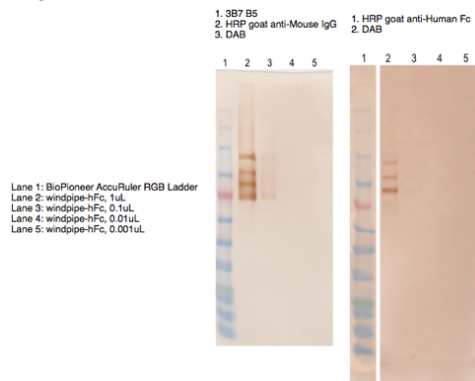


Figure 3.5: Deconvolution assay. Hits from pooled-antigen ELISA are rescreened using a deconvolution assay in which each well contains only one antigen from the bin that produced the original hit. Cross-reactive antibodies will light up multiple wells. Created with BioRender.com

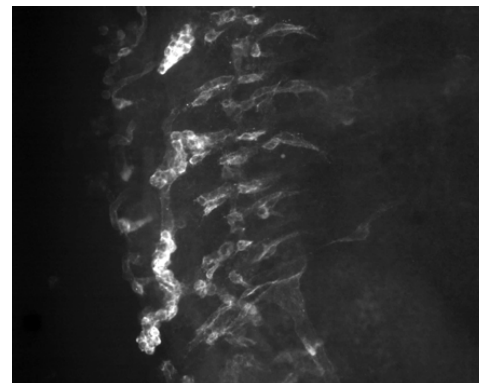
Balb/c 3T3 cells created in Trial 1 were used to inject a cohort of three female Balb/c mice (Figure 3.7). Each mouse was injected with a different number of cells in order to evaluate the effect that cell number had on antibody titer. Each mouse was injected with 1 million, 5 million, or 10 million cells. Sera from immunized mice were obtained after two injections and analyzed for reactivity against soluble forms of the injected antigens on a Western blot. At 1:5,000 (v/v) dilution, the serum from the mouse immunized with 10 million cells showed a broader and stronger antibody response than the other two mice (data not shown). This mouse was injected two

	Single clone?	Original Specificity	wdp	CG4781	CG7702	CD8-Fc	Color Scale
3B7 A1	Yes	CG4781, CG7702, wdp	378100	1049500	289710	473170	6654000
3B7 A7	No	CG4781, CG7702, wdp	5691600	435660	917240	818070	
3B7 B5	Yes	CG4781, CG7702, wdp	5678100	39357	59365	113020	
3B7 C9	Yes	CG4781, CG7702, wdp	935500	87677	571450	221620	
3B7 D4	No	CG4781, CG7702, wdp	6654000	281560	756580	302880	39357
	Single clone?	Original Specificity	EPHA2	EPHA3	EPHA4	CD8-Fc	Color Scale
6F1 B8	No	EPHA2, EPHA3, EPHA4	1080400	313380	261660	224040	1173600
6F1 C4	No	EPHA2, EPHA3, EPHA4	-4	89924	63716	413550	
6F1 F10	Yes	EPHA2, EPHA3, EPHA4	602750	1173600	523300	367420	
6F1 G8	No	EPHA2, EPHA3, EPHA4	1097200	472020	457130	428850	-4
	Single clone?	Original Specificity	AXL	DDR1	TYRO3	ERBB3	Color Scale
7E4 B1	No	AXL, DDR1, TYRO3, ERBB3	267670	253800	840290	281430	949450
7E4 D2	No	AXL, DDR1, TYRO3, ERBB3	5	949450	211380	217380	5

(a) Relative Luminescence Units (RLU) values for the eleven clones designated as hits. 3B7 subclones generally reacted to windpipe (wdp), and 3B7 B5 was the only single clone with high specificity. 6F1 subclones showed cross-reactivity towards all antigens, including the negative control.



(b) Western blots showing reactivity of 3B7 B5 (left) and HRP-conjugated anti-human Fc (right) against windpipe-human Fc. Note the similar staining pattern.



(c) Live-dissected stage 16 embryo stained with anti-windpipe hybridoma supernatant (3B7 B5) at 1:3 (v/v) dilution. Image at 20x magnification.

Figure 3.6: Hybridoma subclone ELISA screening results and 3B7 B5 antibody characterization. HRP = horseradish peroxidase.

additional times for a total of 4 injections over 2 months. The spleen of this mouse was then used for hybridoma production.

A total of 756 hybridoma supernatants were screened using a 19-plex bead set on the Bio-Plex 200 (Figure 3.8). The 19-plex bead set was composed of 7 antigen-coupled regions, 4 human Fc control bead regions (tdTomato-hFc, CD8-hFc, human Fc and human IgG), 4 non-specific binding control regions (GFP-MBP, Bovine IgG, BSA, and baculovirus), and 4 anti-isotype antibody regions. Bovine IgG was included among the protein controls because it co-purified with the human Fc-fusion antigens

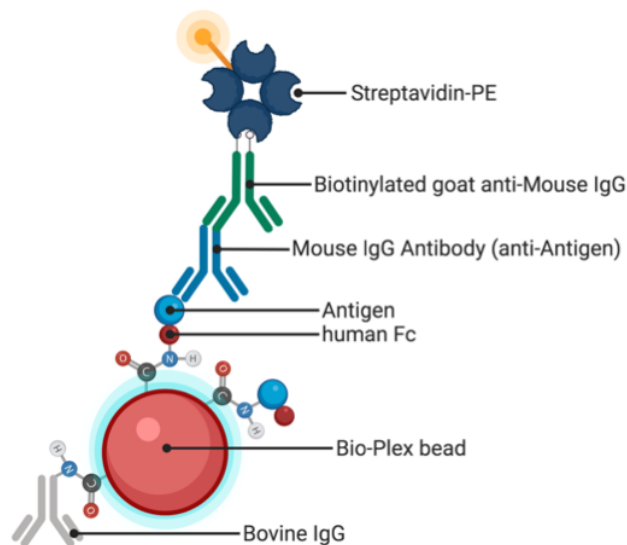
Number	Protein/Annotation ID	Species
1	AXL	<i>H. Sapiens</i>
2	DDR1	<i>H. Sapiens</i>
3	EPHA2	<i>H. Sapiens</i>
4	EPHA3	<i>H. Sapiens</i>
5	EPHA4	<i>H. Sapiens</i>
6	ERBB3	<i>H. Sapiens</i>
7	TYRO3	<i>H. Sapiens</i>

Figure 3.7: List of immunogens overexpressed on the surface of Balb/c 3T3 cell lines injected into female Balb/c 3T3 mice in Trial 2.

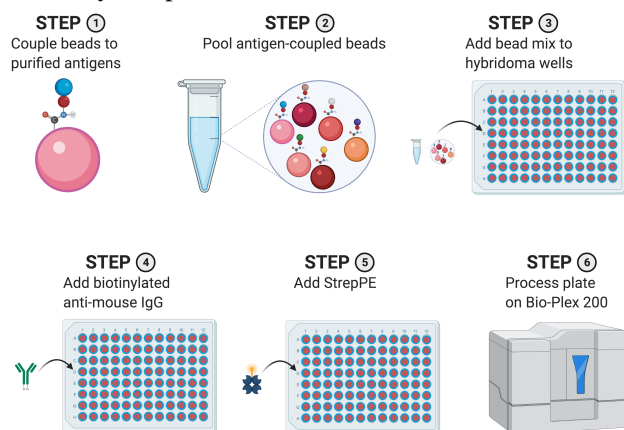
when they were purified from S2 supernatants containing 10% (v/v) fetal bovine serum using Protein A. Therefore, it was necessary to couple bovine IgG to a separate bead region in order to distinguish antigen-specific monoclonal antibodies from those specific to bovine IgG. Hybridoma supernatants containing antibodies against epitopes common to all antigens (i.e. human Fc, the extra amino acids flanking the antigen contributed by the *attB* recombination site, V5 epitope, His₆-tag) were identified as those that produced a signal in all 7 antigen-coupled bead regions. Mouse anti-human IgG (Fc γ specific) (Jackson ImmunoResearch Laboratories Cat. 209-005-098) and PBS were included as positive and negative sample controls, respectively. Out of 756 hybridoma supernatants, 127 were selected for rescreen analysis. A significant number of clones dropped out between the primary screen and the secondary screen, resulting in only 54 out of 127 supernatants being rescreened. EPHA2 appeared to be immunodominant, based on the fact that the majority of antibodies were specific to this antigen (Figure 3.9).

Thirteen clones were selected for large scale growth after the secondary screen. A final Bio-Plex screen was conducted on the supernatants of these 13 clones, along with positive, negative, and isotype controls (Figure 3.10a). Only 1 antigen-specific mAb was identified with high confidence: 18F6. 18F6 showed strong specificity to human EPHA2, despite the fact that it shares high amino acid sequence similarity with two other antigens in the set, namely human EPHA3 and human EPHA4 (Figure 3.11a), and to murine EPHA2 (Figure 3.11b). Isotype data were most reliable from the Jackson goat antibodies, and isotype was determined by using the ratio of the MFIs in these bead regions. 18F6 had an IgG/IgM ratio of 28.28, the highest in the screen, and is therefore most likely an IgG isotype (Figure 3.10b).

The five hybridomas with high IgM/IgG ratios (17A5, 17C3, 18E8, 19B1, and



(a) Antigens fused to human Fc were coupled to Bio-Plex beads. Bovine IgG co-purifies along with antigen-human Fc fusions using Protein A. If hybridoma supernatants contain antibodies specific to antigen, they should bind and get detected using biotinylated anti-Mouse IgG (~25% cross-reactivity to Mouse IgM) followed by StrepPE.



(b) Workflow of semi-automated hybridoma screening using the Bio-Plex. All reagent addition and transfer steps were accomplished using a Tecan Evo 2 liquid handler.

Figure 3.8: Schematic diagram of hybridoma screen via Bio-Plex. StrepPE = streptavidin-phycoerythrin. Created with BioRender.com

22F12) exhibited detectable reactivity towards GFP-MPB, the only protein expressed in *E. coli* in the bead set (Figure 3.10). These results suggest that IgMs may preferentially recognize bacterial glycosylation patterns.

Antigen	# of clones
AXL	9
DDR1	3
EPHA2	22
EPHA3	7
EPHA4	4
ERBB3	5
TYRO3	6
Total	56
Dual-reactive	2
Unique	54

Figure 3.9: Number of clones specific to each antigen in secondary Bio-Plex hybridoma screen.

3.5 Discussion

Immunization of mice with recombinant syngeneic cells has been hypothesized to result in a reduced background immune response compared to recombinant allogeneic or xenogeneic cells (Ebersbach and Geisse, 2012). Dreyer et al. injected HEK cells expressing *Plasmodium falciparum* antigens on their surface into mice and found more hybridomas specific to HEK cell-surface proteins than their target antigens in their cell-based screen (Dreyer et al., 2010). In this study, Balb/c mice were immunized with Balb/c 3T3 cells expressing target antigens on their surface. However, reactivity towards untransfected Balb/c 3T3 cells was not measured. Therefore, further work is needed to evaluate the hypothesis.

The experiments described herein demonstrated that monoclonal antibodies can be successfully generated by immunizing mice with syngeneic, antigen-expressing cells, consistent with previously published studies (Panyutich et al., 1990; Huang et al., 2019). Hybridoma screening with mixed antigen pools was shown to be effective for examining specificity against a large number of analytes using limited volumes of hybridoma supernatants. In addition, a semi-automated hybridoma screening method involving multiplexed suspension bead arrays was established. Using this technology, antibodies can be screened for specificity and isotype of up to 500 analytes simultaneously without deconvolution.

Only one high quality mAb was identified from each fusion experiment. Several factors may have contributed to this result, stemming from the fact that hybridoma production is a highly inefficient process. PEG fusions routinely produce one viable

	Beats															Rockland goat anti-mouse IgM Cat 610-1107	Jackson donkey anti-mouse IgG Cat 715-005-150	Jackson goat anti-mouse IgM Cat 115-005-075	Jackson goat anti-mouse IgG Cat 115-005-164	
	AXL-hFc	DOR1-hFc	TYRO3-hFc	EPHA2-hFc	EPHA3-hFc	EPHA4-hFc	ERBB3-hFc	bovine IgG	GFP-MBP	IdTomato-hFc	CD8-hFc	human Fc	human IgG	BSA	baculovirus					
mouse anti-human 200 ng/mL	4320	24045.5	17457	8053	11269.5	4987.5	17970	510	425	449	335	25738	12558	7449.5	15789	678	7547	333.5	2338.5	
mouse anti-human 20 ng/mL	622	8713	4870	1941	2463	773	5714	150	87	125.5	80	15418	4073	1490.5	5787	120.5	3390.5	99	996.5	
mouse anti-human 2 ng/mL	64	1030	538.5	245	308	71	517	28	42	38	16	2865	563.5	101	3333	34	768.5	23	282	
mouse anti-human 0.2 ng/mL	17	72	49.5	36	50	11.5	56	19	20	22	12	214	48.5	17.5	2994	17	328	14.5	116	
PBS	12.5	34.5	20	36	35	13	31	20	23	28	9.5	192.5	23	14	2988.5	17.5	439	19	94	
PBS	11	38	20.5	34	27	13	30.5	18	19	27	11.5	195.5	24.5	15	2976	18	393	17	114.5	
PBS	14	32	23	34	31.5	7	31.5	15	19	21	9	180.5	23	15.5	3122	16	382	16	190	
PBS	14	28	19	12.5	28	8	24	16	16	20	12	174	22	10	2758	16.5	385	13	134	
16A1	42	110	52	73	38	11	76	26	1380	45	15.5	245	27	20	2955	27.5	3917	577	1226	
16F2	16	25	16	28	27	8	21	16	113.5	15.5	12	126	18	9.5	2866	15.5	281	28	150	
16H6	15	28	16	36	29.5	11	31	19	29.5	20	9	185	21	10.5	3052	12	302	16.5	102	
17A5	15.5	43	31	64	28	9	41	41	3338	33.5	17	152	24	24	2897	22.5	1038	1638	310	
17B3	17	33	24	29.5	17	7	27	17	105	16	14	186.5	22	13	2917	16	1386.5	76	322	
17C3	14	39	36	29.5	39	11.5	34.5	38.5	4930	32.5	18	165.5	38	26.5	2940.5	38	753.5	2301	147	
18E8	13	33	25	32	33	7.5	33	26	2112	25	13	111	26	18.5	2806.5	20	440	906	144	
18F6	25	73.5	84.5	23650	454	99	175.5	84	73.5	55	54	217	66	67	2807	77	3821.5	64.5	1824	
19B1	16	36	25	43	30	8	45	24.5	3846.5	26	15	155	29.5	20	2717	20	792	1487.5	87	
19B8	15	29	23	63	58.5	7	21	17	101	18	9	166	22	13	3107	15	1127	77.5	326	
20A6	13.5	21	17	33	33	8	25	17	44.5	17	13	123	18	10	2902	14	407	30	105	
20H3	13	15	8.5	12.5	12	6	14	15.5	11	16	10	11	6	7	2787	11	23	11	14	
22F12	12	28	20	21	80	5	29.5	21.5	2954	24	14	110	19	16	2709	20	437	1274	73	
Color Scale:	25738															12871.5				5

(a) Heatmap of MFI values of 13 hybridoma subclones, along with positive and negative controls. Green represents high MFI values and white represents low MFI values. Note the strong signal for EPHA2-hFc for hybridoma 18F6.

Sample	Jackson goat anti-mouse IgM Cat 115-005-075	Jackson goat anti-mouse IgG Cat 115-005-164	IgM/IgG ratio	IgG/IgM ratio	Color Scale:
mouse anti-human 200 ng/mL	333.5	2338.5	0.14	7.01	28.28
mouse anti-human 20 ng/mL	99	996.5	0.10	10.07	
mouse anti-human 2 ng/mL	23	282	0.08	12.26	
mouse anti-human 0.2 ng/mL	14.5	116	0.13	8.00	
PBS	19	94	0.20	4.95	
PBS	17	114.5	0.15	6.74	
PBS	16	190	0.08	11.88	
PBS	13	134	0.10	10.31	
16A1	577	1226	0.47	2.12	
16F2	28	150	0.19	5.36	
16H6	16.5	102	0.16	6.18	
17A5	1638	310	5.28	0.19	
17B3	76	322	0.24	4.24	
17C3	2301	147	15.65	0.06	
18E8	906	144	6.29	0.16	
18F6	64.5	1824	0.04	28.28	
19B1	1487.5	87	17.10	0.06	
19B8	77.5	326	0.24	4.21	
20A6	30	105	0.29	3.50	
20H3	11	14	0.79	1.27	
22F12	1274	73	17.45	0.06	0.04

(b) IgM/IgG and IgG/IgM ratios of the MFIs from the Jackson goat anti-isotype-coupled beads. 18F6 produces a strong IgG/IgM ratio.

Figure 3.10: Results from Bio-Plex hybridoma screen.

hybridoma from 10^5 starting cells (Greenfield, 2014), and typical hybridoma fusion protocols call for a ratio of 5 to 10 splenocytes per myeloma cell (Lebrón et al., 1999; Hattori et al., 2015). Because splenocytes fuse at a 1:1 ratio with myeloma cells, 80-90% of splenocytes are discarded during this step. Both of these factors lead to a low B-cell sampling efficiency, which may be insufficient for obtaining antibodies against multiple antigens. Taken together, these data suggest that the hybridoma fusion step itself is a bottleneck toward high-throughput monoclonal antibody production. For these reasons, methods that bypass hybridoma formation, such as B-cell immortalization (Pasqualini and Arap, 2004), and direct B-cell in-

terrogation (Reddy et al., 2010; DeKosky, Ippolito, et al., 2013; DeKosky, Kojima, et al., 2014; Murugan et al., 2015; Starkie et al., 2016; Jahnmatz et al., 2016; Ouisse et al., 2017), have emerged as attractive alternatives.

The antigenicity of the target proteins may have been inadequate to elicit a strong immune response from the mice, especially the human tyrosine kinase receptor extracellular domains which share 93-99% amino acid sequence similarity with the orthologous murine proteins. Indeed, when human and fruit fly proteins were injected together, the majority of hybridoma supernatants contained antibodies specific for fruit fly proteins because of the greater evolutionary distance between flies and mice. However, the fact that we were able to obtain at least one antibody against human EPHA2 demonstrated that sequence similarity does not necessarily exclude an immune response. Lastly, differential growth rates of each antigen-expressing line within the mixed cell population used for immunization may have resulted in underrepresentation of some antigens. Ideally, each line should be individually sorted, grown in sufficient quantities, mixed in well-defined ratios, and frozen to ensure equal representation of each antigen prior to immunization.

Multiplexed immunization and screening will undoubtedly form the basis of high-throughput monoclonal antibody production in the future. Multiplexed bead suspension arrays address several of the technical challenges associated with screening hybridoma supernatants against a large number of analytes and are amenable to automation by robotic liquid handlers. Additionally, this format enables facile identification of antibody isotype and cross-reactivity within a single assay. One of the two monoclonal antibodies generated in this study was shown to perform well in Western blotting and immunohistochemistry, demonstrating that this system is capable of identifying antibodies that are useful in other basic research applications. Hybridoma technology is responsible for ~50 of the 79 U.S. FDA-approved monoclonal antibody therapeutics on the market (Lu et al., 2020). It is therefore critical to continue to optimize immunization and screening methods to ensure that the discovery pipeline remains stable for future generations.

MULTIPLEXED BEAD-BASED INTERACTOME SCREENING

4.1 Background

Cell-surface and secreted proteins (CSSPs) mediate cell adhesion and participate in the reception stage of cellular communication. They also play critical roles in development, where they impart unique identities to cells and serve as guidance cues to other cells in the developing organism. Protein interaction networks, or interactomes, have been the topic of many research papers because these binding events provide clues to a protein's function and underlying biology. The discovery that programmed death-ligand 1 (PD-L1) binds to programmed cell death protein 1 (PD-1) was pivotal in deciphering how these proteins function in the immune system (Freeman et al., 2000; Okazaki and Honjo, 2007). The chemoaffinity hypothesis proposed that assembly of neural circuits involves interactions among cell-surface proteins (Sperry, 1963), and some of these specific interactions have been identified in the visual circuit of the *Drosophila melanogaster* model organism (Carrillo et al., 2015; Menon et al., 2019). As a result, mapping CSSP interaction networks remains a high priority among scientists.

Common PPI detection methods, such as yeast two-hybrid (Y2H) and affinity-purification followed by mass spectrometry (AP/MS), often fail to accurately identify interactions between CSSPs (Wright et al., 2010). Y2H screens, first described in 1989 (Fields and Song, 1989), rely on binary interactions localized to the nuclei of yeast, but this environment is not suitable for proper folding of CSSPs which require an oxidizing environment. However, a modification of Y2H utilizing a split ubiquitin has been described that is applicable to the study of *cis*-interacting membrane proteins (Stagljar et al., 1998) but not secreted proteins. Despite this advancement, one study comparing various PPI detection methods suggested that high-throughput Y2H data have poor quality (Mering et al., 2002). AP/MS is a technique that is useful for detecting protein complexes beyond just binary interactions. Tandem affinity purification followed by mass spectrometry (TAP/MS) was a noteworthy improvement of the method (Rigaut et al., 1999) and was found to have both higher accuracy and broader coverage than other PPI techniques (Mering et al., 2002). Nevertheless, the assay is typically performed on intracellular proteins and is not

well suited for extracellular domains of integral membrane proteins. Cell-free, high-throughput approaches to binary PPI screens utilizing protein microarrays have also been explored (Ramachandran et al., 2008; Braun et al., 2009).

The need for dedicated assays to uncover the CSSP interactome is highlighted by the fact that many of the interactions comprising the network are transient and weak (Merwe and Barclay, 1994). Multimerization of bait or prey proteins has been employed successfully as a strategy to overcome these limitations, suggesting that avidity compensates for low-affinity monomeric interactions. The avidity-based extracellular interaction screen (AVEXIS) utilized pentamerized prey proteins to screen against monomeric bait proteins captured on streptavidin-coated plates (Bushell et al., 2008). The authors showed that pentamerization of prey dramatically enhanced the sensitivity of their assay (Bushell et al., 2008), and the technique was applied in a screen involving nearly 7,600 interactions to construct a zebrafish neuroreceptor interaction network (Söllner and Wright, 2009).

Similar strategies have been applied to study interactomes of other organisms, especially *Drosophila melanogaster*. Wojtowicz et al. exploited clustering of dimeric bait and prey proteins on capture and detection antibodies in a screen of 3,500 pairwise interactions of Dscam isoforms, revealing a preference for homophilic binding among the various isoforms (Wojtowicz, Wu, et al., 2007). Another report chronicled the development of the Extracellular Interactome Assay (ECIA), in which dimerized bait proteins were screened against pentamerized prey proteins (Özkan et al., 2013). Approximately 200 *Drosophila melanogaster* proteins belonging to three different families, namely fibronectin type III, leucine-rich repeat, and immunoglobulin superfamily (IgSF), were assayed for binding in a screen involving over 20,000 pairwise interactions. The study elucidated several highly-connected binding networks, including one among the 21-member defective-in-proboscis-response (Dpr) IgSF subfamily and a previously uncharacterized 9-member IgSF subfamily henceforth known as Dpr-interacting proteins (DIPs). Subsequent studies have further characterized this network, including *in vivo* expression patterns (Tan et al., 2015) and *in vitro* interaction affinities of member proteins (Cosmanescu et al., 2018), and biological significance by highlighting its role in the determination of synaptic specificity during development (Carrillo et al., 2015; Xu et al., 2018; Menon et al., 2019). The ECIA was also applied for interactome screening of *Arabidopsis thaliana* leucine-rich repeat receptor kinases (Smakowska-Luzan et al., 2018). The authors found that pentamerization of the prey proteins was a key requirement for

enhanced detection sensitivity, corroborating the observation from Bushell et. al. A pooled-prey variation of the ECIA was recently used to screen 564 human IgSF cell-surface proteins (Wojtowicz, Vielmetter, et al., 2020). This represents the first step toward the generation of the complete human cell-surface protein interactome.

Microsphere-based multiplex analysis, also known as bead suspension array technology, is a platform well-suited for interactome screening and confers important advantages over previous methodologies. The dynamic range of the microsphere-based assay is many orders of magnitude greater due to its utilization of a fluorescence-based reporter as opposed to the colorimetric reporters of competing assays. The ability to multiplex dramatically reduces the number of wells required for screening, with the reduction given as $n^2 - n$ for an assay involving n analytes.

4.2 Introduction

A genetic screen for mutations affecting neuromuscular specificity in abdominal hemisegments of *Drosophila* embryos revealed that *beaten path* was one of the genes required for normal development (Van Vactor et al., 1993). In *beat* mutants, intersegmental nerve b (ISNb) motor axons fail to defasciculate and innervate muscles 14 and 28 (Fambrough and Goodman, 1996). Another genetic screen conducted by the same laboratory found that *sidestep* produces a similar phenotype (Sink et al., 2001). Cell aggregation studies later showed that Beat interacts with Side, setting the framework for the hypothesis that Beat-expressing motor axons follow a Side-labeled substrate pathway (Siebert et al., 2009). The Beat and Side protein subfamilies were later expanded to 14 and 8 members, respectively, based on bioinformatics (Pipes et al., 2001; Vogel, Teichmann, and Chothia, 2003). However, only one interaction among these protein subfamilies had been detected – that of Beat (now called Beat-Ia) with Side. The Beat-Side interactome emerged from the global ECIA screen (Özkan et al., 2013). These data showed that several Beat subfamily members bind to Side subfamily members.

In 2017, our laboratory published the results of a screen of the Beaten Path-Sidestep interaction network using microsphere-based multiplex analysis. The screen was named the Bio-Plex Interactome Assay (BPIA) after the Bio-Rad Laboratories-branded instrument used to conduct the experiment (Li et al., 2017). The study uncovered three new interactions – Beat-1c::Side-1, Beat-1c::Side-3, and Beat-6::Side-2. In this work, we repeated the Beaten Path-Sidestep interaction screen, but with several modifications intended to enhance sensitivity. First, we removed

alkaline phosphatase (AP) from the COMP-fusion expression vector since AP activity is not used as a reporter in the bead-based assay. Second, we expressed proteins in the Expi293 expression system and purified them using NiNTA-affinity chromatography, in order to concentrate each bait and prey as much as possible. Third, we replaced streptavidin with avidin in the bait immobilization step. Fourth, we incorporated positive and negative controls for both bait and prey, to assess how concentration of each sample would affect identification of hits.

Lastly, we tested Protein A as a bait capture reagent, to create an assay more closely resembling the ECIA. The bait/prey configuration in the BPIA is opposite to the ECIA: pentameric COMP-AP proteins were bound to streptavidin-coupled beads as baits, and dimeric Fc proteins were used as prey. By running BPIA-like assays in both configurations, we hoped to determine whether it was important to use higher-order multimers as prey. Intuitively, one might think that this would be the case because avidity enhancement is created by dense binding of baits to the surface of beads. Maximum avidity (and therefore perhaps sensitivity) should be attained by using the higher-order multimers as prey and dimers as bait. However, our results show that this is not the case.

4.3 Materials and Methods

Plasmid construction. Beat and Side pCR8 entry vectors were created as previously described (Özkan et al., 2013). Expression plasmids were created by Gateway LR recombination using Gateway® LR Clonase™ II Enzyme Mix (Life Technologies Cat. 11791-020) into modified destination vectors based on the pcDNA™ backbone. Modifications to the pcDNA backbone included a hemagglutinin signal peptide, a Gateway recombination cassette, HRV 3C protease site, multimerization domain, C-terminal tags (V5 or FLAG®, AviTag™ and His₆-tag), and Hepatitis B virus post-transcriptional regulatory element (HPRE). Two multimerization domains were utilized: Fc tag from human IgG1 coupled with V5 epitope for dimerization and rat cartilage oligomatrix proteins (COMP) coupled with FLAG® epitope for pentamerization.

For *in vivo* biotinylation, a pCR8 entry vector containing the gene for *E. coli* biotin ligase (BirA) containing the KDEL ER-retention sequence (Tykvar et al., 2012) followed immediately by a stop codon was first created by TOPO TA cloning, and an expression construct was then generated by Gateway LR recombination.

Protein expression and purification. Proteins were expressed using the Expi293™

Expression System (ThermoFisher Scientific) according to standard protocols. Supernatants were collected 4 days after transfection and proteins were purified over 1 mL HisTrap FF columns (GE Healthcare) using 10 mM imidazole in the binding buffer, 20 mM imidazole in the wash buffer, and 250 mM imidazole in the elution buffer. Protein quality and purity was determined by SDS-PAGE and Western blot against the V5 epitope for the Fc-fusion proteins and the FLAG epitope for the biotinylated COMP proteins. The following proteins were not detected on Western blot: Beat6-hFc-V5, Side7-hFc-V5, Beat4-COMP-FLAG, Beat6-COMP-FLAG, Side3-COMP-FLAG, and Side7-COMP-FLAG.

In vivo biotinylation was performed by co-transfecting the plasmid encoding BirA in a 1:1 mass ratio with the plasmid encoding the target protein. The extent of biotinylation was estimated by electrophoretic mobility shift assay using unboiled avidin (Sigma-Aldrich Cat. A9275) or streptavidin (Sigma-Aldrich Cat. S4762) in SDS-PAGE.

Coupling of Bio-Plex beads. Approximately 62,500 Bio-Plex Pro™ Magnetic COOH Beads were coupled to 12 µg of avidin (Sigma-Aldrich Cat. A9275), streptavidin (Sigma-Aldrich Cat. S4762), Protein A (Rockland™ Antibodies and Assays Cat. PA00-00), or goat anti-human IgG (Fcγ specific) (Jackson ImmunoResearch Laboratories Cat. 109-005-098) using the Bio-Plex Amine Coupling Kit (Bio-Rad Laboratories Cat. 171-406001). PBS was used as the bead wash buffer, storage buffer, and staining buffer. The blocking buffer was 2.5% (w/v) bovine serum albumin (BSA) solution prepared from lyophilized BSA (Rockland™ Antibodies and Assays Cat. BSA-1000) in TBST with 0.01% (w/v) thimerosal. Each reaction was performed in a 1.5 mL microcentrifuge tube. For each step, beads were briefly vortexed, spun at maximum speed in an Eppendorf 5424 at room temperature for 30 seconds, and immobilized on a DynaMag™-2 Magnet (ThermoFisher Scientific Cat. 12321D) for 2 minutes before removal of the supernatant. This procedure was used for all subsequent staining and washing steps.

Bait-loading onto coupled beads. Approximately 25,000 coupled beads were re-suspended with 100 µL of NiNTA-purified protein baits. One bead region was assigned to each bait. Fc-fusion bait proteins were mixed with Protein A-coupled beads and biotinylated COMP-fusion bait proteins were mixed with avidin-coupled beads. Mouse anti-FLAG mAb (Sigma-Aldrich Cat. F3165) and sheep anti-Biotin Ab (Bethyl Laboratories Cat. A150-110A) were diluted 1:50 (v/v) into 1x PBS and included as baits for Protein A-coupled beads. Biotinylated chicken anti-human Fc

(Thermo Fisher Scientific Cat. SA1-72048) was loaded onto avidin-coupled beads at concentration of 20 ng/ μ L in 1x PBS. Beads were incubated at room temperature for 3 hours with gentle agitation. Following the bait loading period, the beads were washed once with PBS and then combined to create a multiplexed bait mixture.

Interactome screen. The bait-loaded, multiplexed beads were pipetted into microcentrifuge tubes containing 100 μ L of NiNTA-purified preys or controls. Controls for the avidin-coupled beads were mouse anti-FLAG mAb (Sigma-Aldrich Cat. F3165) diluted 1:50 (v/v) in 1x PBS and mouse anti-His mAb (GenScript Cat. A00186-100) at 2 ng/ μ L in 1x PBS. Biotinylated chicken anti-human Fc (Thermo Fisher Scientific Cat. SA1-72048) at 20 ng/ μ L in 1x PBS was included as a prey for the Protein A-coupled beads. Preys were incubated with bait-loaded beads for 4-6 hours at room temperature with gentle agitation. The beads were then washed with PBS and prey-specific detection reagents were added to the beads. Streptavidin-phycoerythrin (Bio-Rad Laboratories Cat. 171-304501) diluted to 1x with PBS was used to detect biotinylated COMP-fusion prey proteins. Mouse anti-V5-tag Antibody (BioLegend Cat. 680601) at 500 ng/ μ L in PBS followed by goat anti-mouse IgG-PE (Santa Cruz Biotechnology Cat. sc-3738) diluted 1:400 (v/v) in PBS was used to detect V5-tagged human Fc-fusion prey proteins. Each detection reagent was incubated for 30 minutes at room temperature. Beads were washed with PBS after each incubation. The beads were resuspended in 100 μ L of PBS, transferred to a 96-well microplate (Bio-Rad Laboratories Cat. HSP9631), and analyzed on the Bio-Plex 200 instrument. The read method was set to count 50 beads per region per well.

Data analysis. Raw data from the Bio-Plex runs were exported as Microsoft Excel worksheets and all subsequent analyses were performed in Excel. Blank subtraction was performed by subtracting the MFIs of each bait::prey interaction by the MFIs of the corresponding bait::mock pure negative control. Negative values after blank subtraction were filtered out. The remaining MFIs were divided by the corresponding bait::mouse anti-His or bait::mouse anti-FLAG MFIs to express the data relative to each of the two positive controls, essentially normalizing it by setting each positive control to 1. Lastly, each bait::prey normalized data point was divided by its corresponding mCherry::prey normalized data point to express the data as fold-change over background. Side7-hFc-V5 was the only prey to drop out during the final data processing step due to the fact that the mCherry MFI at this prey became negative after blank subtraction. However, Side7-hFc-V5 was only one of six proteins that

failed to be detected on Western blot. Therefore, data from the other five proteins that failed to express, namely Beat6-hFc-V5, Beat4-COMP-FLAG, Beat6-COMP-FLAG, Side3-COMP-FLAG, and Side7-COMP-FLAG, were also discarded. For histogram analysis, all drop-outs and discarded data were assigned a value of 0.

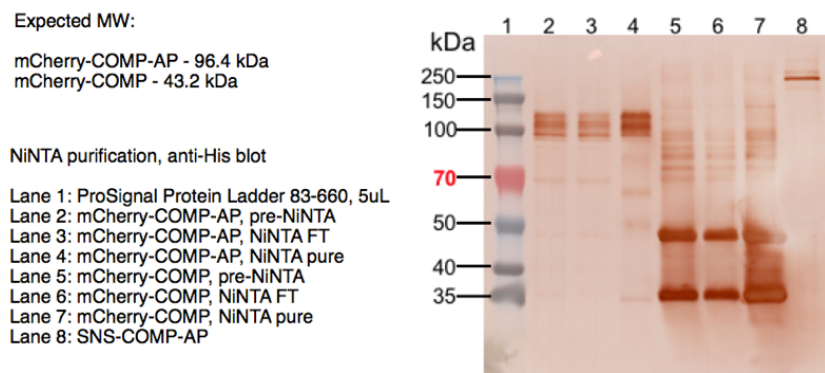
4.4 Results

Removing AP improves expression. Because the COMP-AP fusion proteins expressed poorly in both the ECIA and the BPIA, we sought to improve expression of these proteins by removing the relatively large AP gene from the expression vector. AP activity was used as the assay reporter in the ECIA, but the Bio-Plex uses a fluorescent reporter, rendering the AP useless in this context. The fluorescent protein mCherry was expressed in Expi293 cells in two secreted forms – mCherry-COMP-His₆ or mCherry-COMP-AP-His₆. The supernatants were then purified using nickel affinity chromatography. Purification efficiency was monitored using Western blot or fluorescence measurement. The mCherry-COMP-His₆ produced a much stronger signal on the Western blot than mCherry-COMP-AP-His₆ (Figure 4.1a), indicating that mCherry-COMP-His₆ was expressed at a higher level than mCherry-COMP-AP-His₆. Fluorescence measurements of the mCherry expressions, taken at three different stages of purification, showed overall higher relative fluorescence units (RFUs) from the mCherry-COMP-His₆ than mCherry-COMP-AP-His₆ (Figure 4.1b). We concluded from these data that removing AP improves expression.

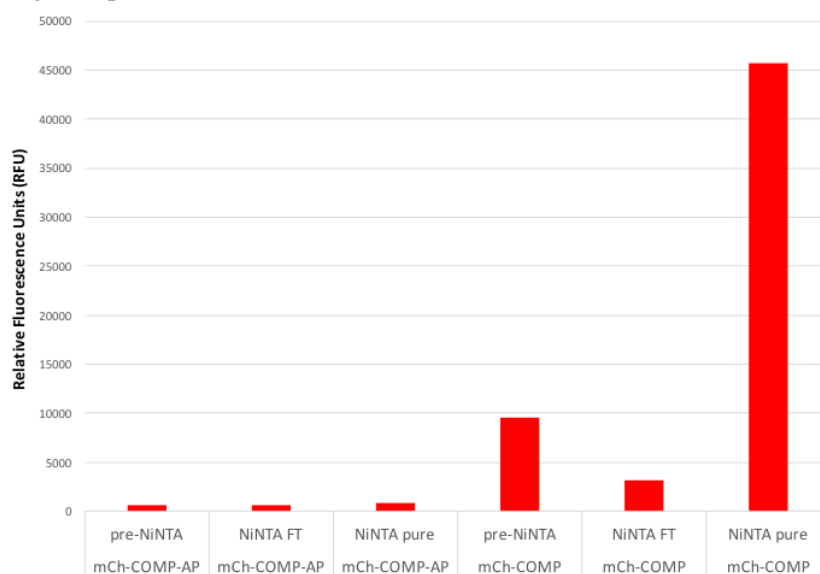
Bead-based interactome screen: bead count. The bead count and MFI data for both capture methods were organized into a table and analyzed. Per-region bead count ranged from 11 to 329 and 20 to 252 for avidin-coupled and Protein A-coupled formats, respectively (data not shown). Only one sample in both runs triggered a low bead count warning – mock pure in the avidin-coupled format.

Bead-based interactome screen: controls. Beat-Side interactome screening was conducted using two bait-loading strategies. Biotinylated COMP fusions were captured using avidin-coupled beads (Figure 4.2a) whereas human Fc fusions were captured using Protein A-coupled beads (Figure 4.2b). PBS and mock pure controls were included among both baits and preys.

The extent of biotinylated COMP-fusion bait capture on avidin-coupled beads was measured using mouse anti-His and mouse anti-FLAG as preys. Mouse anti-His showed lower signal in the negative control beads (PBS and mock pure) than mouse



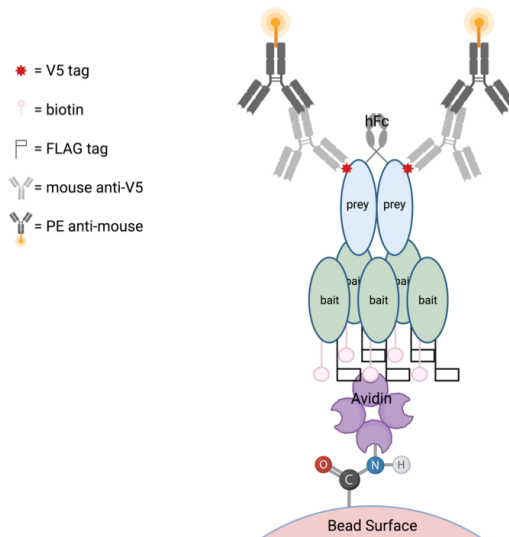
(a) Anti-His Western blot depicting signal of His-tagged protein at three stages of purification.



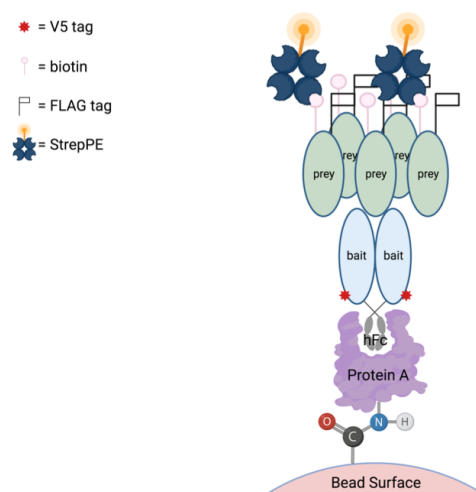
(b) Fluorescence intensity of mCherry at three stages of purification using excitation wavelength of 587 nm and emission wavelength of 610 nm.

Figure 4.1: Comparison of expression of mCherry-COMP-AP-His₆ versus mCherry-COMP-His₆. FT = flowthrough.

anti-FLAG. The relative concentration of each human Fc-fusion prey was measured using beads directly coupled to Protein A and goat anti-human Fc, or biotinylated chicken anti-human Fc loaded onto an avidin-coupled bead. There was potential conflict in using Protein A in this context because of potential binding to the mouse anti-V5 IgG2b and PE-conjugated goat anti-mouse detection antibodies in the assay design. However, Protein A binds weakly to mouse IgG2b and total goat IgG. Nevertheless, these data were ultimately not used to determine relative prey concentration, despite good agreement with goat anti-human Fc data (Figure 4.3a). Goat anti-human Fc produced higher signals than biotinylated chicken anti-human Fc



(a) Avidin capture of biotinylated bait.

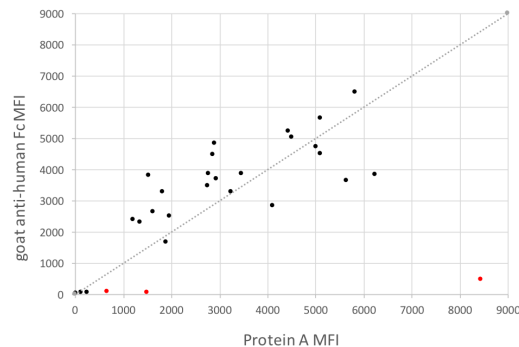


(b) Protein A capture of human Fc-fused bait.

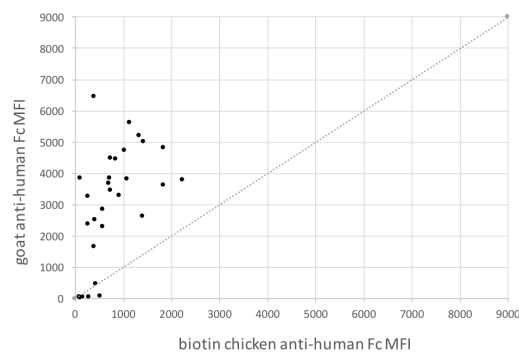
Figure 4.2: Schematic diagram of bead-based interactome screening. PE = phycoerythrin. Created with BioRender.com

for almost every prey tested (Figure 4.3b). We concluded that goat anti-human Fc was the best reagent for measuring relative concentration of human Fc-fusion preys (Figure 4.4a).

The extent of human Fc-fusion bait capture on Protein A-coupled beads was measured using biotinylated chicken anti-human Fc. Chicken IgY was selected because it shows no binding to Protein A, and the reagent needed to be biotinylated in order to be recognized by the streptavidin-phycoerythrin detection reagent. Unfortunately, the antibody produced high signal in every bead, including the negative controls



(a) Correlation among MFIs generated by human Fc-fusion preys on goat anti-human Fc- or Protein A-coupled beads. Goat anti-human Fc produced higher signals, on average, than Protein A. The three data points in red depict mouse IgG1 preys, where Protein A signal would be expected to be higher. Excluding the red data points, a Pearson's correlation coefficient of 0.78 was calculated from these data.



(b) Correlation among MFIs generated by human Fc-fusion preys on goat anti-human Fc-coupled beads or avidin-coupled beads loaded with biotinylated chicken anti-human Fc. Nearly every prey generated a higher signal on goat anti-human Fc-coupled beads. A Pearson's correlation coefficient of 0.44 was calculated from these data.

Figure 4.3: Comparison of detection of human Fc fusion prey proteins via bead-coupled goat anti-human Fc, bead-coupled Protein A, or bead-coupled avidin incubated with biotinylated chicken anti-human Fc. Gray dotted lines represent the line $y = x$. MFI = median fluorescence intensity.

(PBS and mock pure), at the tested concentration. We therefore had no choice but to exclude these data in the final analysis. The relative concentration of each bi-

	Avidin:biotin chicken anti- hFc	Protein A	goat anti-hFc
Avidin:biotin chicken anti- hFc	1.00		
Protein A	0.28	1.00	
goat anti-hFc	0.44	0.78	1.00

(a) Correlation coefficients of three different bead-coupled reagents used to measure MFIs of human Fc-fusion preys.

	mouse anti-FLAG	sheep anti-biotin	avidin	streptavidin
mouse anti-FLAG	1.00			
sheep anti-biotin	0.97	1.00		
avidin	0.60	0.54	1.00	
streptavidin	0.96	0.89	0.71	1.00

(b) Correlation coefficients of four different bead-coupled reagents used to measure MFIs of biotinylated, FLAG-tagged preys. Mouse anti-FLAG and sheep anti-biotin had the highest correlation at 0.97, followed closely by 0.96 between mouse anti-FLAG and streptavidin.

Figure 4.4: Comparison of correlation coefficients of reagents used to detected prey proteins in two different paradigms of interactome screening. MFI = median fluorescence intensity.

otinylated COMP-fusion prey was measured using beads directly coupled to mouse anti-FLAG, sheep anti-biotin, avidin, and streptavidin. Correlation coefficients between every pair of reagents were calculated from the MFI data of all the preys (Figure 4.4b).

Bead-based interactome screen: Beat-Side network. The raw MFI data from both runs were organized into a 2-color heat map (Figure 4.5). Visualized in this manner, avidin-capture identified eight strong interactions and Protein A-capture identified four (Figure 4.6). All four of the strong interactions identified by the Protein A-capture method were also identified in the avidin-capture method. Of the remaining eight unique interactions, only one was orientation-independent, meaning the interaction was detected in both directions. The phenomenon of orientation-dependent binding was also seen in the ECIA and the previous BPIA, and its exact causes are unknown. However, they may be related to the concentration of one of the proteins within the pairwise interaction, especially when the protein is acting as prey. The observation that a greater number of strong binding events were obtained using

avidin-capture may reflect the fact that human Fc-fusion proteins expressed at higher levels, on average, than the biotinylated COMP proteins. Further corroboration of this hypothesis is given by the fact that most of the strong binding interactions were observed with Side proteins as human Fc-fusion prey since they expressed far better as human-Fc fusions than as biotinylated COMP-fusions. Standardization of the concentrations of each bait and prey before conducting an interactome screen may begin to address this problem, but this step is generally seen as far too cumbersome for such assays, especially at higher scales. Figure 4.5 also illustrated that the issue of “sticky” preys was more problematic in the Protein A-capture method than in the avidin-capture method, seen in the heat map as green rows. For these reasons, we decided to proceed with data analysis of the avidin-capture run only.

		Avidin capture																				Protein A capture														
Prey #	Prey name	beatt1	beatt2	beatt3	beatt4	beatt5	beatt6	beatt7	beatt8	beatt9	beatt10	beatt11	beatt12	beatt13	beatt14	beatt15	beatt16	beatt17	beatt18	beatt19	beatt20	side1	side2	side3	side4	side5	side6	side7	side8	mCherry	mock prep	PBS	mouse anti-FLAG	sheep anti-beitin	avidin	streptavidin
1	beat 1a Hc-V5-His	128	377.5	184	214	100	301	265	185	240.5	118	86	216	283	82	164	324	185.5	62	171	55	179	42	158	1937	703	1937	703	567	724	43115.5	2343				
2	beat 1b Hc-V5-His	102	204	126.5	145	83	235	186	129	209.5	107	59	146.5	168	59	73	347	146	57	181.5	51.5	131	39	151.5	1556	284.5	272	224.5	3249	3284						
3	beat 1c Hc-V5-His	303.5	618	256	467	304.5	586	522	397	343	293	206.5	374	531	336.5	133	578	344	103.5	362.5	110	228	83	288	2240	1856	1842.5	1673	2909	4816						
4	beat 2a Hc-V5-His	305.5	627	308	454	368	489	567.5	392	444.5	305	287	486	492	316.5	349.5	373.5	435	334.6	351	94	335	205	312	2339.5	3122	1401	1415	4514	5022						
5	beat 2b Hc-V5-His	291	564.5	375	480.5	345	604	687.5	436	436	304	200	345	498	120	4357	715	370	547.6	316	119	211	59	227	1816.5	1177	1072.5	990.5	282	6235	3825.5					
6	beat 3a Hc-V5-His	270	350	267	309	167	412.5	348	269	284	183	117	253	330	66.5	101	243	216	70	186	67	205.5	38	169	1934.5	660	706	713	2395	3682.5						
7	beat 3b Hc-V5-His	212	463	231	450	193.5	413.5	542.5	402.5	355	253	155.5	290	389	30	85.5	528	282	115.5	318	94	170	60	281.5	1797	795	2033	2392	5008.5	4730						
8	beat 3c Hc-V5-His	318.5	622	202	384	299	270	411	288	279	217	203	209	380	100.5	80.5	377	257	94	264	354.5	248	37	202	2200	830.5	736	875.5	5098.5	4503.5						
9	beat 4 Hc-V5-His	170	376	206	264.5	155.5	259	333	216	276	180	115.5	225	305	97	104.5	340.5	207	89	321	141	388	57.5	192	1857.5	626	738	550	2762	3463						
10	beat 5a Hc-V5-His	333	626	437	500	346	657	612	316	393	263	271	545	499	157	138	341.5	358.5	139.5	395	3690	299.5	79.5	306.5	1735	1523	1138	1384	5098	5635						
11	beat 5b Hc-V5-His	451	640	408	427	432	607	576	591	591	406	410	500	611	352.5	208.5	692	417	358	418	969	391	96	297.5	2325.5	1587	1311.5	1670	4481	5212						
12	beat 5c Hc-V5-His	199.5	377	250	270.5	237.5	397	544	333	304	211	119	230	336.5	92	99	267.5	193	72	166	6852	182.5	60	227	1432	623.5	726	597.5	2769.5	3857						
13	beat 6 Hc-V5-His	184	355	230.5	279	123	318	226	214	366.5	173	86	248	376	49.5	73	288	229.5	81	261	53	254	45	153	3491	518	403	612.5	5829	6456						
14	beat 7 Hc-V5-His	173.5	361.5	244	274	233	303	370.5	199	206	186.5	151	217	314	104.5	100	207	234	93	266	74	142.5	45	227	882	419	395	411	1886.5	1655						
15	side 1 Hc-V5-His	820	891.5	520	1265	938	532.5	747	737	609	673.5	674.5	585	1068	520.5	321	1403	1064	367.5	780.5	273	650.5	313	689	1954.5	1680	1410.5	1738.5	1629	5236						
16	side 2 Hc-V5-His	236.5	491	415	461	296	417	697	394	387	259	179	142	388	179	178	315.5	297.5	175	260	178	267.5	104	300	1765	885	914	877.5	1826	3288						
17	side 3 Hc-V5-His	187.5	426	281.5	268	140	337	363.5	262	329	176	97	229	322	63	105.5	1251	218	79	336	71	188	63	176	1992	943	843	952	2867.5	4457						
18	side 4 Hc-V5-His	175	325.5	181	441.5	325	273	241	249	179.5	146	82	182	330	65	102	418	209.5	65	209	73.5	154.5	68.5	163	1558	417	415	445	1961	2510.5						
19	side 5 Hc-V5-His	374	808	328.5	557	440	551	700.5	517	535.5	433	218	173	470	130	166.5	360	294.5	138	270.5	128	224	83	345	2097	1984	2235	1841	1534	3797						
20	side 6 Hc-V5-His	207	430.5	250	287	181	395	421.5	237	255	529	568	289	339	98	101	482	230	139	243.5	86	180	71	262	1577	778	569	617.5	1531	2304						
21	side 7 Hc-V5-His	111	178	162.5	165	43.5	193	162	140	274	104	43	127	251	36	44	188	143	48.5	100	30	201	34.5	119	3076	114	101	122.5	3468	3846						
22	side 8 Hc-V5-His	101	219	153	137	90	156.5	157	140	365	101	57	100	223.5	47	75.5	223.5	132.5	51.5	149	43	123	33	147.5	1496	356	269.5	358	1206	2388						
23	mCherry Hc-V5-His	269	411	239	396.5	203	308.5	382	413	275	206.5	184.5	268	545.5	212.5	138.5	341	323	74	193	131	219.5	79.5	286	1753	2198	1834.5	2109	5645.5	3641						
24	mock prep	120	195	179	134.5	45	166	107	125	198	132.5	38	96	187	21	35	127	117.5	53.5	101	39	169	30	121	2775	123	87	157	252	47						
25	PBS	56	136	115	79	75	101	72	101	72	101	72	101	72	101	72	101	72	101	72	101	72	101	72	101	72	101	72	101	72	101	72				
26	mouse anti-FLAG	5931	6227	6425	6890	6348	5952	8195	7491	7167	5417	5492	6020	4772	8205	3462	5065	4929	4546	4454	3008	6693	3680	8893	4923.5	1020	513.5	111	1371	671.5	82.5					
27	mouse anti-His	1080	4008	4742	3385	2922	2199	5368	4223	1877	2349	2019	2198	1477	4492	1248	1775	1976	1800	2030	1068	3383	1180	5734.5	244.5	334	157	349	1495	46						

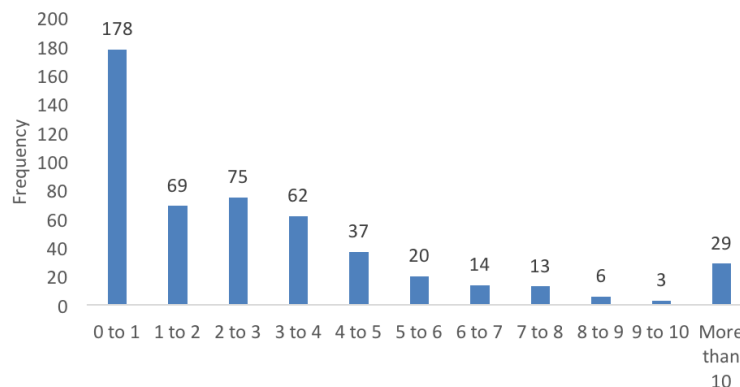
Prey #	Prey name	beatt1	beatt2	beatt3	beatt4	beatt5	beatt6	beatt7	beatt8	beatt9	beatt10	beatt11	beatt12	beatt13	beatt14	beatt15	beatt16	beatt17	beatt18	beatt19	beatt20	side1	side2	side3	side4	side5	side6	side7	side8	mCherry	mock prep	PBS	mouse anti-FLAG	sheep anti-beitin	avidin	streptavidin
1	beat1a COMP-FLAG-monobio-His	76	49.5	38	55	45	69	48	69	53	49	53	45	94.5	29	59.5	53.5	59	39.5	48.5	49	274	43	67	234	272	431	379.5	55	76						
2	beat1b COMP-FLAG-monobio-His	42.5	28	24	40.5	27	43	25	44	45	27	30	29	97	19	31	33	25.5	24	31	27	382	22	39	132	411	967.5	718	713	136						
3	beat1c COMP-FLAG-monobio-His	197.5	97	73	90	76	102	106	123	92	101	86	88.5	244.5	65	128	95	62	63	67	101	654.5	65.5	114	582	744	1282.5	1012	579	428						
4	beat2a COMP-FLAG-monobio-His	103	58.5	57.5	84	69.5	68	60.5	61.5	60	58	59	65	144	35	83	54	52	142.5	70	53.5	407	48.5	73.5	318.5	392	785	619	359	158						
5	beat2b COMP-FLAG-monobio-His	782	330	406	651.5	611	904.5	638	710	590.5	520	658	569.5	976	371.5	886	425.5	382	332.5	548.5	517.5	1070	379.5	673	3988	1461	2374	1735.5	2525	1539						
6	beat3a COMP-FLAG-monobio-His	117	76	62	99	70.5	117	74	106	111	81	115	77	177.5	45.5	88	64	73.5	60	89	74	609	67	110	492	604.5	875.5	786	1050	132						
7	beat3b COMP-FLAG-monobio-His	104	87	70.5	93.5	92	111.5	86	106	94	80	86	74	169	53.5	89	56.5	97	47.5	68.5	90	471	65	105	410.5	513	1070	826	978	1154						
8	beat3c COMP-FLAG-monobio-His	59	27.5	25.5	66	50	62.5	52.5	70	64.5	28	44	47	95.5	32	50	46.5	44	37.5	53	48	281	28.5	65	242.5	295	839	517	291	1215.5						
9	beat4 COMP-FLAG-monobio-His	84.5	48	42	64	45.5	66	57	59	56.5	54.5	46	42	149	38.5	55	60	61	36	39.5	50	549.5	39.5	70	474	578.5	756	735	55	61						
10	beat5a COMP-FLAG-monobio-His	305.5	182	175	239	202.5	190	182.5	224	176	177	204	178	346	94.5	211	147	185.5	156	210.5	345.5	819	145	256	744.5	897	1564.5	1269	522	468.5						
11	beat5b COMP-FLAG-monobio-His	3288	1984	2896	2789	2052	2188	1939	2453	2536	2541	2273	2607	2988	1910	2286	1896	1627	1854	3246	3444	2772	1783	2748	2597	3970	5115	4348	1936.5	3806.5						
12	beat5c COMP-FLAG-monobio-His	200	132	134.5	195	133.5	159	136.5	161.5	132	127.5	145	145	243	90	123.5	88	100	131	152	177	498	79	163.5	451	636	878.5	752	321	159						
13	beat6 COMP-FLAG-monobio-His	34	24.5	19	30	27	36	26	30.5	35	27.5	25.5	30	81	19	32	28	30	19	27.5	25	314	25	36	244.5	290	532	450.5	92	42						
14	beat7 COMP-FLAG-monobio-His	2046	1596	1744	1619	1639	1843	1708	1311	1742	1614	1659	1385	2205	1593	1394	1539	1734	1858	1232	1779	2344	1228	1817	2426	2790	3483	2637	2789	2628						
15	side 1 COMP-FLAG-monobio-His	809	464.5	513	941.5	765	627																													

Avidin-capture	Protein A-capture
beat5b::side6	beat5b::side6
side1::beat2a	
side1::beat2b	
side4::beat2a	
side4::beat2b	side4::beat2b
side6::beat5a	side6::beat5a
side6::beat5b	side6::beat5b
side6::beat5c	

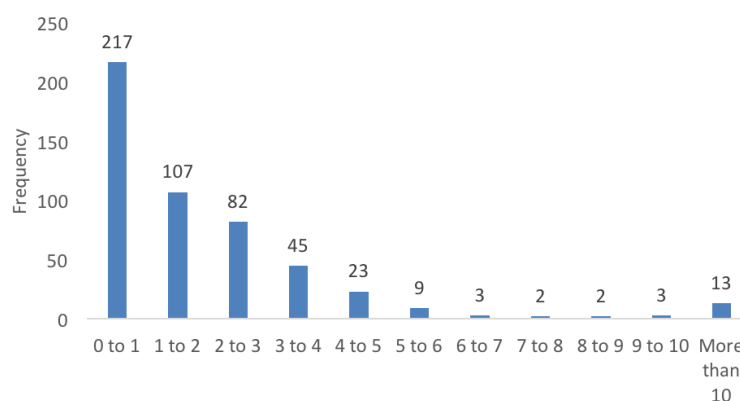
Figure 4.6: List of strong pairwise binding interactions in the Beat-Side interactome. Four interactions were detected using both capture methods. Interactions detected in both orientations in both bait-capture formats are highlighted in yellow. Interactions are listed according to bait::prey.

determined by the number of interactions in the “0 to 1” and “More than 10” categories for each antibody. There are several reasons that can explain this result. First, the FLAG-tag is a larger and more well-defined epitope than the His₆-tag so the antibodies generated against the former will have reduced background compared to the latter. Second, there may be secreted proteins in Expi293 cell culture media that co-purify with His-tagged proteins using nickel-based affinity chromatography. These contaminants may have short stretches of histidine residues that cause them to bind to nickel resin, similar to what is observed in the *E. coli* expression system (Robichon et al., 2011). The mouse anti-His antibody may be recognizing these proteins immobilized on the beads, producing non-specific signal unrelated to the beat or side proteins. Fold-change over background data derived from mouse anti-FLAG-normalized signal data was used to score beat::side interactions.

Two new Beat-Side interaction maps were created using the top 13 and 23 hits from the screen, and they were compared to our last iteration of the Beat-Side interaction map (Figure 4.8). The top 13 values were chosen because their fold-change over background values were greater than 10 and because there are currently 13 Beat-Side interactions defining the network (Li et al., 2017). In theory, the top 13 hits from this screen should fully recapitulate the interaction map. An additional 10 interactions were selected to populate a second interaction map using a threshold of >6 fold-change over background. Importantly, the 23-hit interaction map identified the known Beat 1a:Side 1 interaction and deorphanized Beat 1b, Beat 3a, Beat 3c, Side 5, and Side 8. The map appeared to also "reorphanize" Beat 6 and Side 7, but these proteins did not express well in our hands. Therefore, no conclusions about



(a) Blank-subtracted MFIs >0 were normalized to mouse anti-His then divided by background mCherry-COMP.



(b) Blank-subtracted MFIs >0 were normalized to mouse anti-FLAG then divided by background mCherry-COMP. Mouse anti-FLAG was more stringent in weeding out non-binders.

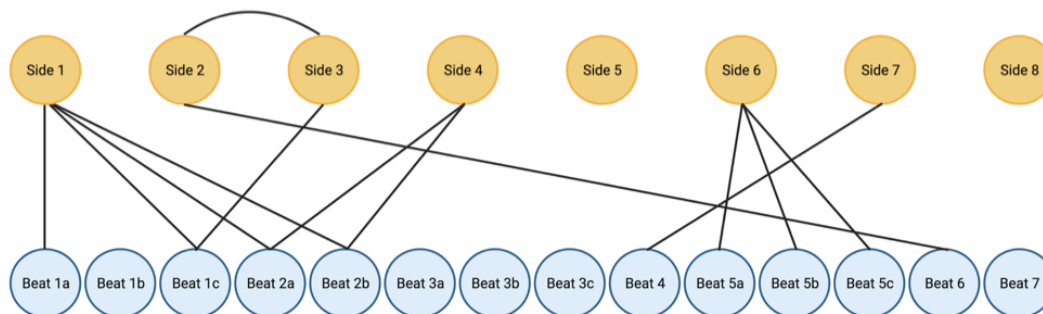
Figure 4.7: Histograms of fold-change over background of the Beat-Side interactome. MFI = median fluorescence intensity.

interactions of Beat 6 and Side 7 should be drawn from this study.

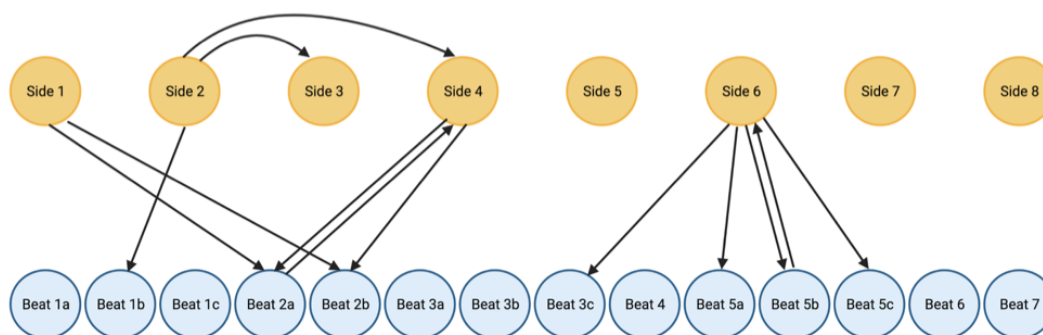
4.5 Discussion

Multiplexed bead-based assays are well-suited for interactome screening. This format is capable of screening a large number of analytes while consuming small volumes of sample. Because each bead is uniquely identifiable, there is no need for cumbersome downstream deconvolution assays.

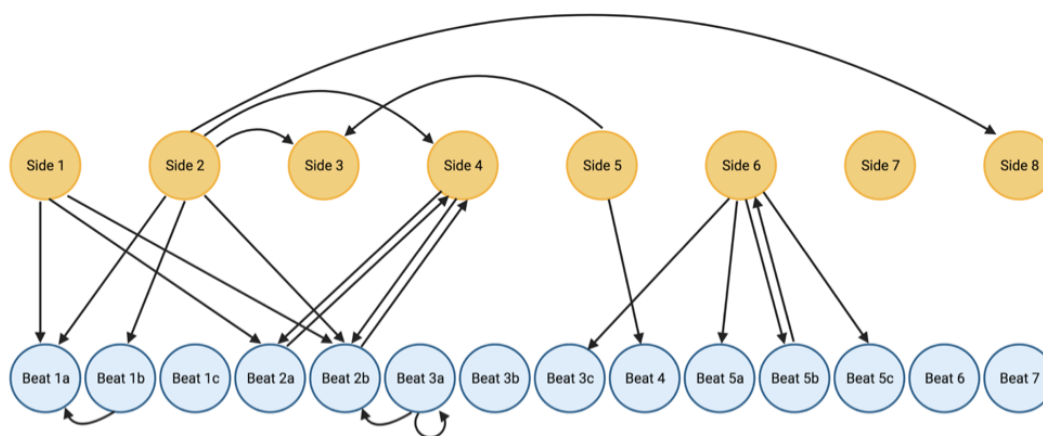
In this work, a subset of the *Drosophila* IgSF superfamily of cell-surface and secreted proteins, the 14-member Beat family and 8-member Side family were screened using a multiplexed bead-based assay. Although this screen had been previously conducted using this format, the work described here utilized a number of modifica-



(a) Original BPIA (2017)



(b) Current BPIA map using 10-fold over background.



(c) Current BPIA map using 6-fold over background.

Figure 4.8: Beat-Side interaction networks determined by suspension bead assay. Current BPIA maps depict monodirectional binding as bait \rightarrow prey and bidirectional binding as bait \leftrightarrow prey. Created with BioRender.com

tions intended to enhance assay sensitivity. As a result, three Beat proteins and two Side proteins were deorphanized using a fold-change over background threshold of >6 , which is markedly higher than the two-fold over background threshold used to score hits in a recent interactome screen on human proteins (Wojtowicz, Vielmetter, et al., 2020).

The identification of new hits via modification of screening methods is only the first step toward validation of these new interactions. Our collaborators plan to conduct a surface plasmon resonance (SPR) analysis on all members of the Beat-Side network. SPR analysis represents current the “gold standard” for validation of binding. These data allow an evaluation of screening methods to determine which methods produce the best identification of true positives while minimizing false positives, similar to published data for the Dpr/DIP interaction network (Cosmanescu et al., 2018). This is important because in very large-scale screens such as the human IgSF interactome, complete human CSSP interactome, or complete *Drosophila* CSSP interactome, it is not practical to assess every interaction by SPR. Accordingly, we need to define methods that will accurately assess binding interactions. The Beat/Side interactome, as currently described, has members with no binding partners within the network. However, the precedent of the Dpr-ome (Cosmanescu et al., 2018) and phylogenetic analysis of the *beat* and *side* genes predict that every protein in the network should have a binding partner within the network. Given the small size of this network, this prediction can be tested by SPR. Our goal in developing these bead-based assays, which is still an active process in our laboratory, is to define a high-throughput screening method that can recover all interactions that are detectable through the labor-intensive SPR methods.

As greater emphasis is placed on high-throughput techniques, scientists are embarking on increasingly ambitious projects requiring the collection of significant amounts of data. Multiplexed bead-based assays fit well within this paradigm, as they can be adapted for both nucleic acid and protein measurements.

BIBLIOGRAPHY

- Balazs, Alejandro B., Jesse D. Bloom, et al. (2013). “Broad protection against influenza infection by vectored immunoprophylaxis in mice”. In: *Nature Biotechnology* 31.7, pp. 647–652. DOI: 10.1038/nbt.2618.
- Balazs, Alejandro B., Joyce Chen, et al. (2012). “Antibody-based protection against HIV infection by vectored immunoprophylaxis”. In: *Nature* 481.7379, pp. 81–84. DOI: 10.1038/nature10660.
- Behjati, Sam and Patrick S. Tarpey (2013). “What is next generation sequencing?” In: *Archives of disease in childhood - Education & practice edition* 98.6, pp. 236–238. DOI: 10.1136/archdischild-2013-304340.
- Bloom, Joshua S. et al. (2020). “Swab-Seq: A high-throughput platform for massively scaled up SARS-CoV-2 testing”. In: *medRxiv* 382, pp. 2158–47. DOI: 10.1101/2020.08.04.20167874.
- Braun, Pascal et al. (2009). “An experimentally derived confidence score for binary protein-protein interactions”. In: *Nature Methods* 6.1, pp. 91–97. DOI: 10.1038/nmeth.1281.
- Burnette, W. Neal (1981). ““Western Blotting”: Electrophoretic Transfer of Proteins from Sodium Dodecyl Sulfate-Polyacrylamide Gels to Unmodified Nitrocellulose and Radiographic Detection with Antibody and Radioiodinated Protein A”. In: *Analytical Biochemistry* 112, pp. 195–203. DOI: 10.1016/0003-2697(81)90281-5.
- Bushell, K. Mark et al. (2008). “Large-scale screening for novel low-affinity extracellular protein interactions”. In: *Genome Research* 18.4, pp. 622–630. DOI: 10.1101/gr.7187808.
- Carrillo, Robert A. et al. (2015). “Control of Synaptic Connectivity by a Network of Drosophila IgSF Cell Surface Proteins”. In: *Cell* 163.7, pp. 1770–1782. DOI: 10.1016/j.cell.2015.11.022.
- Carson, R. T. and Dario A. A. Vignali (1999). “Simultaneous quantitation of 15 cytokines using a multiplexed flow cytometric assay”. In: *Journal of Immunological Methods* 227.1, pp. 41–52. DOI: 10.1016/S0022-1759(99)00069-1.
- Castellani, Aldo (1913). “Typhoid-Paratyphoid Vaccination with Mixed Vaccines”. In: *British Medical Journal* 2.2764, pp. 1577–1578. DOI: 10.1136/bmj.2.2764.1577.
- Castellani, Aldo (1915). “Combined Vaccinations.” In: *The Indian Medical Gazette* 50.11, pp. 406–416. DOI: PMID:PMC5150069.
- Chambers, Ross S. (2005). “High-throughput antibody production”. In: *Current Opinion in Chemical Biology* 9.1, pp. 46–50. DOI: 10.1016/j.cbpa.2004.10.011.

- Chen, Peter, Aruz Mesci, and James R. Carlyle (2011). “CELLISA: Reporter Cell-Based Immunization and Screening of Hybridomas Specific for Cell Surface Antigens”. In: *Methods in Molecular Biology* 748, pp. 209–225. DOI: 10.1007/978-1-61779-139-0_15.
- Chiarella, Pieranna and Vito Michele Fazio (2008). “Mouse monoclonal antibodies in biological research: strategies for high-throughput production”. In: *Biotechnology Letters* 30.8, pp. 1303–1310. DOI: 10.1007/s10529-008-9706-5.
- Chiarella, Pieranna, Melanie Leuener, et al. (2011). “Comparison and Critical Analysis of Robotized Technology for Monoclonal Antibody High-Throughput Production”. In: *Biotechnology Progress* 27.2, pp. 571–576. DOI: 10.1002/btpr.564.
- Coons, Albert H., Hugh J. Creech, and R. Norman Jones (1941). “Immunological Properties of an Antibody Containing a Fluorescent Group.” In: *Experimental Biology and Medicine* 47.2, pp. 200–202. DOI: 10.3181/00379727-47-13084P.
- Cosmanescu, Filip et al. (2018). “Neuron-Subtype-Specific Expression, Interaction Affinities, and Specificity Determinants of DIP/Dpr Cell Recognition Proteins”. In: *Neuron* 100.6, 1385–1400.e6. DOI: 10.1016/j.neuron.2018.10.046.
- De Masi, Federico et al. (2005). “High throughput production of mouse monoclonal antibodies using antigen microarrays”. In: *Proteomics* 5.16, pp. 4070–4081. DOI: 10.1002/pmic.200401279.
- DeKosky, Brandon J., Gregory C. Ippolito, et al. (2013). “High-throughput sequencing of the paired human immunoglobulin heavy and light chain repertoire”. In: *Nature Biotechnology* 31.2, pp. 166–169. DOI: 10.1038/nbt.2492.
- DeKosky, Brandon J., Takaaki Kojima, et al. (2014). “In-depth determination and analysis of the human paired heavy- and light-chain antibody repertoire”. In: *Nature Medicine* 21.1, pp. 86–91. DOI: 10.1038/nm.3743.
- Dreyer, Anita M. et al. (2010). “An efficient system to generate monoclonal antibodies against membrane-associated proteins by immunisation with antigen-expressing mammalian cells”. In: *BMC Biotechnology* 10, p. 87. DOI: 10.1186/1472-6750-10-87.
- Ebersbach, Hilmar and Sabine Geisse (2012). “Antigen generation and display in therapeutic antibody drug discovery - a neglected but critical player”. In: *Biotechnology Journal* 7.12, pp. 1433–1443. DOI: 10.1002/biot.201200066.
- ENCODE Project Consortium et al. (2012). “An integrated encyclopedia of DNA elements in the human genome”. In: *Nature* 489.7414, pp. 57–74. DOI: 10.1038/nature11247.
- Engvall, Eva and Peter Perlmann (1971). “Enzyme-linked immunosorbent assay (ELISA): Quantitative assay of immunoglobulin G”. In: *Immunochemistry* 8.9, pp. 871–874. DOI: 10.1016/0019-2791(71)90454-X.

- Fambrough, Douglas and Corey S. Goodman (1996). "The *Drosophila beaten path* Gene Encodes a Novel Secreted Protein That Regulates Defasciculation at Motor Axon Choice Points". In: *Cell* 87.6, pp. 1049–1058. DOI: 10.1016/S0092-8674(00)81799-7.
- Fields, Stanley and Ok-kyu Song (1989). "A novel genetic system to detect protein-protein interactions". In: *Nature* 340.6230, pp. 245–246. DOI: 10.1038/340245a0.
- Freeman, Gordon J. et al. (2000). "Engagement of the PD-1 Immunoinhibitory Receptor by a Novel B7 Family Member Leads to Negative Regulation of Lymphocyte Activation". In: *Journal of Experimental Medicine* 192.7, pp. 1027–1034. DOI: 10.1084/jem.192.7.1027.
- Fulton, R. Jerrold et al. (1997). "Advanced multiplexed analysis with the FlowMetrix™ system". In: *Clinical Chemistry* 43.9, pp. 1749–1756. DOI: PMID:9299971.
- Gasper, William C. et al. (2014). "Fully automated high-throughput chromatin immunoprecipitation for ChIP-seq: Identifying ChIP-quality p300 monoclonal antibodies". In: *Scientific Reports* 4, p. 5152. DOI: 10.1038/srep05152.
- Gilmour, David S. and John T. Lis (1984). "Detecting protein-DNA interactions *in vivo*: Distribution of RNA polymerase on specific bacterial genes". In: *Proceedings of the National Academy of Sciences* 81.14, pp. 4275–4279. DOI: 10.1073/pnas.81.14.4275.
- Graham, Hilary, Don J. Chandler, and Sherry A. Dunbar (2019). "The genesis and evolution of bead-based multiplexing". In: *Methods* 158, pp. 2–11. DOI: 10.1016/j.ymeth.2019.01.007.
- Greenfield, Edward A., ed. (2014). *Antibodies: A Laboratory Manual*. Second Edition. New York: Cold Spring Harbor Laboratory Press. 847 pp. ISBN: 978-1-936113-81-1.
- Hamilton, Paul M. (1945). "Combined Immunization: Against Whooping Cough, Diphtheria, and Tetanus." In: *The American Journal of Nursing* 45.12, pp. 1024–1025. DOI: PMID:21006552.
- Hattori, Tatsuya et al. (2015). "Successful acquisition of a neutralizing monoclonal antibody against a novel neutrophil-activating peptide, mitocryptide-1". In: *Biochemical and Biophysical Research Communications* 463.1, pp. 54–59. DOI: 10.1016/j.bbrc.2015.05.016.
- Herzenberg, Leonore A., Stephen C. De Rosa, and Leonard A. Herzenberg (2000). "Monoclonal antibodies and the FACS: complementary tools for immunobiology and medicine". In: *Immunology Today* 21.8, pp. 383–390. DOI: 10.1016/S0167-5699(00)01678-9.
- Huang, Chien-Chiao et al. (2019). "Use of syngeneic cells expressing membrane-bound GM-CSF as an adjuvant to induce antibodies against native multi-pass transmembrane protein". In: *Scientific Reports*, pp. 1–11. DOI: 10.1038/s41598-019-45160-9.

- Hudziak, R. M. et al. (1989). “p185^{HER2} Monoclonal Antibody Has Antiproliferative Effects In Vitro and Sensitizes Human Breast Tumor Cells to Tumor Necrosis Factor”. In: *Molecular and Cellular Biology* 9.3, pp. 1165–1172. DOI: 10.1128/mcb.9.3.1165-1172.1989.
- Huff, Janice L. et al. (2002). “*Drosophila windpipe* codes for a leucine-rich repeat protein expressed in the developing trachea”. In: *Mechanisms of Development* 111.1, pp. 173–176. DOI: 10.1016/S0925-4773(01)00609-8.
- International Human Genome Sequencing Consortium et al. (2001). “Initial sequencing and analysis of the human genome”. In: *Nature* 409.6822, pp. 860–921. DOI: 10.1038/35057062.
- Jahnmatz, Peter et al. (2016). “An antigen-specific, four-color, B-cell FluoroSpot assay utilizing tagged antigens for detection”. In: *Journal of Immunological Methods* 433, pp. 23–30. DOI: 10.1016/j.jim.2016.02.020.
- Keij, J. F. and J. A. Steinkamp (1998). “Flow Cytometric Characterization and Classification of Multiple Dual-Color Fluorescent Microspheres Using Fluorescence Lifetime”. In: *Cytometry* 33.3, pp. 318–323. DOI: PMID:9822342.
- Kettman Jr, John R. et al. (1998). “Classification and Properties of 64 Multiplexed Microsphere Sets”. In: *Cytometry* 33.2, pp. 234–243. DOI: PMID:9773885.
- Klein, Florian et al. (2012). “HIV therapy by a combination of broadly neutralizing antibodies in humanized mice”. In: *Nature* 492.7427, pp. 118–122. DOI: 10.1038/nature11604.
- Köhler, Georges and César Milstein (1975). “Continuous cultures of fused cells secreting antibody of predefined specificity”. In: *Nature* 256.5517, pp. 495–497. DOI: 10.1038/256495a0.
- Lebrón, José A. et al. (1999). “Tolerization of adult mice to immunodominant proteins before monoclonal antibody production”. In: *Journal of Immunological Methods* 222.1, pp. 59–63. DOI: 10.1016/S0022-1759(98)00179-3.
- Li, Hanqing et al. (2017). “Deconstruction of the beaten Path-Sidestep interaction network provides insights into neuromuscular system development”. In: *eLife* 6. DOI: 10.7554/eLife.28111.
- Lu, Ruei-Min et al. (2020). “Development of therapeutic antibodies for the treatment of diseases”. In: *Journal of Biomedical Science* 27.1, pp. 1–30. DOI: 10.1186/s12929-019-0592-z.
- Maloney, David G. et al. (1997). “IDEC-C2B8 (Rituximab) Anti-CD20 Monoclonal Antibody Therapy in Patients With Relapsed Low-Grade Non-Hodgkin’s Lymphoma”. In: *Blood* 90.6, pp. 2188–2195. DOI: 10.1182/blood.V90.6.2188.
- Menon, Kaushiki P. et al. (2019). “Interactions between Dpr11 and DIP- γ control selection of amacrine neurons in *Drosophila* color vision circuits”. In: *eLife* 8. DOI: 10.7554/eLife.48935.

- Mering, Christian von et al. (2002). “Comparative assessment of large-scale data sets of protein-protein interactions”. In: *Nature* 417.6887, pp. 399–403. DOI: 10.1038/nature750.
- Merwe, P. Anton van der and A. Neil Barclay (1994). “Transient intercellular adhesion: the importance of weak protein-protein interactions”. In: *Trends in Biochemical Sciences* 19.9, pp. 354–358. DOI: 10.1016/0968-0004(94)90109-0.
- Mesci, Aruz and James R. Carlyle (2007). “A rapid and efficient method for the generation and screening of monoclonal antibodies specific for cell surface antigens”. In: *Journal of Immunological Methods* 323.1, pp. 78–87. DOI: 10.1016/j.jim.2007.02.007.
- Mullis, Kary B. and Fred A. Faloona (1987). “Specific Synthesis of DNA *in Vitro* via a Polymerase-Catalyzed Chain Reaction”. In: *Methods in Enzymology* 155, pp. 335–350. DOI: 10.1016/0076-6879(87)55023-6.
- Murugan, Rajagopal et al. (2015). “Direct high-throughput amplification and sequencing of immunoglobulin genes from single human B cells”. In: *European Journal of Immunology* 45.9, pp. 2698–2700. DOI: 10.1002/eji.201545526.
- Okazaki, Taku and Tasuku Honjo (2007). “PD-1 and PD-1 ligands: from discovery to clinical application”. In: *International Immunology* 19.7, pp. 813–824. DOI: 10.1093/intimm/dxm057.
- Oliver, Kerry G., John R. Kettman, and R. Jerrold Fulton (1998). “Multiplexed Analysis of Human Cytokines by Use of the FlowMetrix System”. In: *Clinical Chemistry* 44.9, pp. 2057–2060. DOI: PMID:9733011.
- Ouisse, Laure-Hélène et al. (2017). “Antigen-specific single B cell sorting and expression-cloning from immunoglobulin humanized rats: a rapid and versatile method for the generation of high affinity and discriminative human monoclonal antibodies”. In: *BMC Biotechnology* 17.1, p. 3. DOI: 10.1186/s12896-016-0322-5.
- Özkan, Engin et al. (2013). “An Extracellular Interactome of Immunoglobulin and LRR Proteins Reveals Receptor-Ligand Networks”. In: *Cell* 154.1, pp. 228–239. DOI: 10.1016/j.cell.2013.06.006.
- Panyutich, Alexander V. et al. (1990). “The Use of Syngeneic Cells Producing Human Somatotrophic Hormone (hSTH) for Immunization of Mice and Development of Hybridomas”. In: *Hybridoma* 9.4, pp. 401–406. DOI: 10.1089/hyb.1990.9.401.
- Pasqualini, Renata and Wadih Arap (2004). “Hybridoma-free generation of monoclonal antibodies”. In: *Proceedings of the National Academy of Sciences* 101.1, pp. 257–259. DOI: 10.1073/pnas.0305834101.
- Pipes, G. C. et al. (2001). “The Beat generation: a multigene family encoding IgSF proteins related to the Beat axon guidance molecule in *Drosophila*”. In: *Development* 128.22, pp. 4545–4552. DOI: 10.1242/dev.128.22.4545.

- Ramachandran, Niroshan et al. (2008). “Next-generation high-density self-assembling functional protein arrays”. In: *Nature Methods* 5.6, pp. 535–538. DOI: 10.1038/nmeth.1210.
- Reddy, Sai T. et al. (2010). “Monoclonal antibodies isolated without screening by analyzing the variable-gene repertoire of plasma cells”. In: *Nature Biotechnology* 28.9, pp. 957–961. DOI: 10.1038/nbt.1673.
- Rigaut, Guillaume et al. (1999). “A generic protein purification method for protein complex characterization and proteome exploration”. In: *Nature Biotechnology* 17.10, pp. 1030–1032. DOI: 10.1038/13732.
- Robichon, Carine et al. (2011). “Engineering *Escherichia coli* BL21(DE3) Derivative Strains To Minimize *E. coli* Protein Contamination after Purification by Immobilized Metal Affinity Chromatography”. In: *Applied and Environmental Microbiology* 77.13, pp. 4634–4646. DOI: 10.1128/AEM.00119-11.
- Saiki, Randall K. et al. (1985). “Enzymatic Amplification of β -globin Genomic Sequences and Restriction Site Analysis for Diagnosis of Sickle Cell Anemia”. In: *Science* 230.4732, pp. 1350–1354. DOI: 10.1126/science.2999980.
- Sanger, F., S. Nicklen, and A. R. Coulson (1977). “DNA sequencing with chain-terminating inhibitors”. In: *Proceedings of the National Academy of Sciences* 74.12, pp. 5463–5467. DOI: 10.1073/pnas.74.12.5463.
- Sauer, Louis W. and Winston H. Tucker (1942). “Simultaneous Administration of Diphtheria Toxoid and Pertussis Vaccine in Young Children”. In: *American Journal of Public Health and the Nation's Health* 32.4, pp. 385–388. DOI: 10.2105/ajph.32.4.385.
- Scheid, Johannes F. et al. (2016). “HIV-1 antibody 3BNC117 suppresses viral rebound in humans during treatment interruption”. In: *Nature* 535.7613, pp. 556–560. DOI: 10.1038/nature18929.
- Siebert, Matthias et al. (2009). “*Drosophila* motor axons recognize and follow a Sidestep-labeled substrate pathway to reach their target fields”. In: *Genes & Development* 23.9, pp. 1052–1062. DOI: 10.1101/gad.520509.
- Siegel, Scott A. et al. (1995). “The Mouse/Human Chimeric Monoclonal Antibody cA2 Neutralizes TNF In Vitro and Protects Transgenic Mice from Cachexia and TNF Lethality In Vivo”. In: *Cytokine* 7.1, pp. 15–25. DOI: 10.1006/cyto.1995.1003.
- Sink, Helen et al. (2001). “*sidestep* Encodes a Target-Derived Attractant Essential for Motor Axon Guidance in *Drosophila*”. In: *Cell* 105.1, pp. 57–67. DOI: 10.1016/s0092-8674(01)00296-3.
- Smakowska-Luzan, Elwira et al. (2018). “An extracellular network of *Arabidopsis* leucine-rich repeat receptor kinases”. In: *Nature* 553.7688, pp. 342–346. DOI: 10.1038/nature25184.

- Söllner, Christian and Gavin J. Wright (2009). “A cell surface interaction network of neural leucine-rich repeat receptors”. In: *Genome Biology* 10.9, R99. DOI: 10.1186/gb-2009-10-9-r99.
- Sperry, R. W. (1963). “Chemoaffinity in the Orderly Growth of Nerve Fiber Patterns and Connections”. In: *Proceedings of the National Academy of Sciences* 50.4, pp. 703–710. DOI: 10.1073/pnas.50.4.703.
- Stagljar, Igor et al. (1998). “A genetic system based on split-ubiquitin for the analysis of interactions between membrane proteins *in vivo*”. In: *Proceedings of the National Academy of Sciences* 95.9, pp. 5187–5192. DOI: 10.1073/pnas.95.9.5187.
- Starkie, Dale O. et al. (2016). “Generation of Recombinant Monoclonal Antibodies from Immunised Mice and Rabbits via Flow Cytometry and Sorting of Antigen-Specific IgG⁺ Memory B Cells”. In: *PLoS ONE* 11.3, e0152282. DOI: 10.1371/journal.pone.0152282.
- Staudt, Nicole, Nicole Müller-Siennerth, and Gavin J. Wright (2014). “Development of an antigen microarray for high throughput monoclonal antibody selection”. In: *Biochemical and Biophysical Research Communications* 445.4, pp. 785–790. DOI: 10.1016/j.bbrc.2013.12.033.
- Tan, Liming et al. (2015). “Ig Superfamily Ligand and Receptor Pairs Expressed in Synaptic Partners in *Drosophila*”. In: *Cell* 163.7, pp. 1756–1769. DOI: 10.1016/j.cell.2015.11.021.
- Tokuyama, H. (1975). “*In Vitro* Proliferative Response of BALB/c Mouse Spleen Cells Stimulated with Trinitrophenylated Syngeneic Spleen Cells”. In: *Immunology* 29.5, pp. 875–884. DOI: PMID:PMC1445988.
- Towbin, Harry, Theophil Staehelin, and Julian Gordon (1979). “Electrophoretic transfer of proteins from polyacrylamide gels to nitrocellulose sheets: Procedure and some applications”. In: *Proceedings of the National Academy of Sciences* 76.9, pp. 4350–4354. DOI: 10.1073/pnas.76.9.4350.
- Tykvart, J. et al. (2012). “Efficient and versatile one-step affinity purification of *in vivo* biotinylated proteins: Expression, characterization and structure analysis of recombinant human glutamate carboxypeptidase II”. In: *Protein Expression and Purification* 82.1, pp. 106–115. DOI: 10.1016/j.pep.2011.11.016.
- Van Vactor, David et al. (1993). “Genes That Control Neuromuscular Specificity in *Drosophila*”. In: *Cell* 73.6, pp. 1137–1153. DOI: 10.1016/0092-8674(93)90643-5.
- Venter, J. Craig et al. (2001). “The Sequence of the Human Genome”. In: *Science* 291.5507, pp. 1304–1351. DOI: 10.1126/science.1058040.
- Vignali, Dario A. A. (2000). “Multiplexed particle-based flow cytometric assays”. In: *Journal of Immunological Methods* 243.1, pp. 243–255. DOI: 10.1016/S0022-1759(00)00238-6.

- Vogel, Christine, Sarah A. Teichmann, and Cyrus Chothia (2003). “The immunoglobulin superfamily in *Drosophila melanogaster* and *Caenorhabditis elegans* and the evolution of complexity”. In: *Development* 130.25, pp. 6317–6328. DOI: 10.1242/dev.00848.
- Wojtowicz, Woj M., Jost Vielmetter, et al. (2020). “A Human IgSF Cell-Surface Interactome Reveals a Complex Network of Protein-Protein Interactions”. In: *Cell* 182.4, 1027–1043.e17. DOI: 10.1016/j.cell.2020.07.025.
- Wojtowicz, Woj M., Wei Wu, et al. (2007). “A Vast Repertoire of Dscam Binding Specificities Arises from Modular Interactions of Variable Ig Domains”. In: *Cell* 130.6, pp. 1134–1145. DOI: 10.1016/j.cell.2007.08.026.
- Wright, Gavin J. et al. (2010). “High-throughput identification of transient extracellular protein interactions”. In: *Biochemical Society Transactions* 38.4, pp. 919–922. DOI: 10.1042/BST0380919.
- Xu, Shuwa et al. (2018). “Interactions between the Ig-Superfamily Proteins DIP- α and Dpr6/10 Regulate Assembly of Neural Circuits”. In: *Neuron* 100.6, 1369–1384.e6. DOI: 10.1016/j.neuron.2018.11.001.
- Yu, Zhe et al. (2010). “High-Throughput Antibody Generation Using Multiplexed Immunization and Immunogen Array Analysis”. In: *Journal of Biomolecular Screening* 15.10, pp. 1260–1267. DOI: 10.1177/1087057110380045.